Sensor and Simulation Notes

Note 242

September 1977

Some Analysis of EC-135 Aircraft Model Data

Valdis V. Liepa
Thomas B. A. Senior
University of Michigan
Ann Arbor, Michigan 48109

Abstract

Over the last few years the surface currents and charges have been measured on a variety of scale model aircraft using sweep frequency techniques. Four topics bearing on these data are examined in this report. They are: the smoothing of data to remove experimental noise, the assessment of model-lead interactions on charge data, the effect of HF wire antennas on the frequency response of the EC-135, and the manner in which fields are excited on the shadowed side of cylinders.

TABLE OF CONTENTS

1. INTRODUCTION

In a previous technical report [1] on this contract, data were presented for the surface currents and charges measured on a small scale model of the EC-135 aircraft. The data were obtained using a model 1/216 in scale in combination with the overlapping frequency ranges 0.45 to 1.10, 1.00 to 2.20 and 2.00 to 4.25 GHz to simulate the full scale range 2.1 to 19.7 MHz. As with our study of the F-111 aircraft [2], it was required that the raw data be presented, and because of the need to submit these as soon as they were obtained, it was not possible to include in [1] any analysis or discussion of the data.

We here examine four topics relevant not only to the EC-135 model data but to most of our other surface field measurements as well. They are, in the order of presentation:

(a) smoothing of the data to remove experimental noise,

(b) assessment of the effect of model-lead interaction on charge data,

(c) effect of HF wire antennas on the frequency response of the EC-135,

---

1. Valdis V. Liepa, "Surface Field Measurements on Scale Model EC-135 Aircraft for ACHILLES I and II Data Interpretation," Interaction Application Memo 14, 1977.

2. Valdis V. Liepa, "Surface Field Measurements on Scale Model F-111 Aircraft," Interaction Application Memo 13, 1977.

and (d) study of the excitation of fields on the shadowed side of cylinders. A FORTRAN listing of the program used to smooth the data is given in Appendix A, and Appendix B contains some additional data pertinent to topic (d).

2. DATA SMOOTHING

No measurement no matter how carefully performed yields data which are 100 percent accurate; and in practice there are always errors caused by the non-ideal nature of the measuring instrument, thermal noise, human fallibility, etc. This is certainly true in the case of surface field measurements; and among the numerous possible sources of error are the reflection of energy from the chamber walls, discontinuities in cables and connectors, interaction between the model and the sensor leads, frequency drift of the signal source, and the instability of the pre-amplifier and network analyzer with temperature and time. In a typical measured frequency response curve such as that shown in Figure 1, it is clear that most of the small wiggles are not real and are due to one or more of the above sources of error. Nevertheless, there are exceptions: the null at 3.5 MHz is believed real and is even more pronounced for the current measured on the top of the fuselage (see Figure 6 of [1]).

The high frequency oscillations can be removed by numerically smoothing the data with a low pass filter algorithm for complex-valued data. The method used is based on the nth order system governed by [3]

---

3. James A. Cadzow, Discrete-Time Systems, Prentice-Hall, Inc., Englewood Cliffs, New Jersey, 1973.

$$y(k) = \frac{1}{2}(1 - \alpha)[u(k) + u(k - 1)] + \alpha y(k - 1)$$

with $$\alpha = \frac{1}{a}\left(b - \sqrt{b^2 - a^2}\right) ,$$

$$a = 2^{1/n}(1 + \cos \omega_1 T) ,$$

and $$b = a + 2(1 - \cos \omega_1 T) ,$$

where input and output data sets are u and y, respectively, the order of the system is n, the bandwidth is ω_1 and the sampling time is T. As written, the equations are for processing a time sequence of numbers, but were adapted to process numbers as a function of frequency by changing the time variable to frequency. To avoid the frequency delay which occurs when data are passed through a low pass filter, the program was written to filter the data twice; first in the direction of increasing frequency and then backwards, to give an n = 2 filtering effect for n = 1 input. The other input parameter is f_c. This is related to the cut-off frequency of the filter and representative of the number of oscillations passed through the filter for each data set, three of which make up a given figure. A FORTRAN listing of the program is given in Appendix A.

The results of filtering the data of Figure 1 using n = 2 (effective) and f_c = 20 and 5 are shown in Figures 2 and 3 respectively. As expected, the filtering does remove the small wiggles and improve the appearance of the data, but it also tends to remove such real features as the null at 3.5 MHz. It is therefore clear that filtering is a technique which should only be used with the utmost discretion; and because of the danger that it may remove valid characteristics, filtering was not applied to the data in [1, 2].

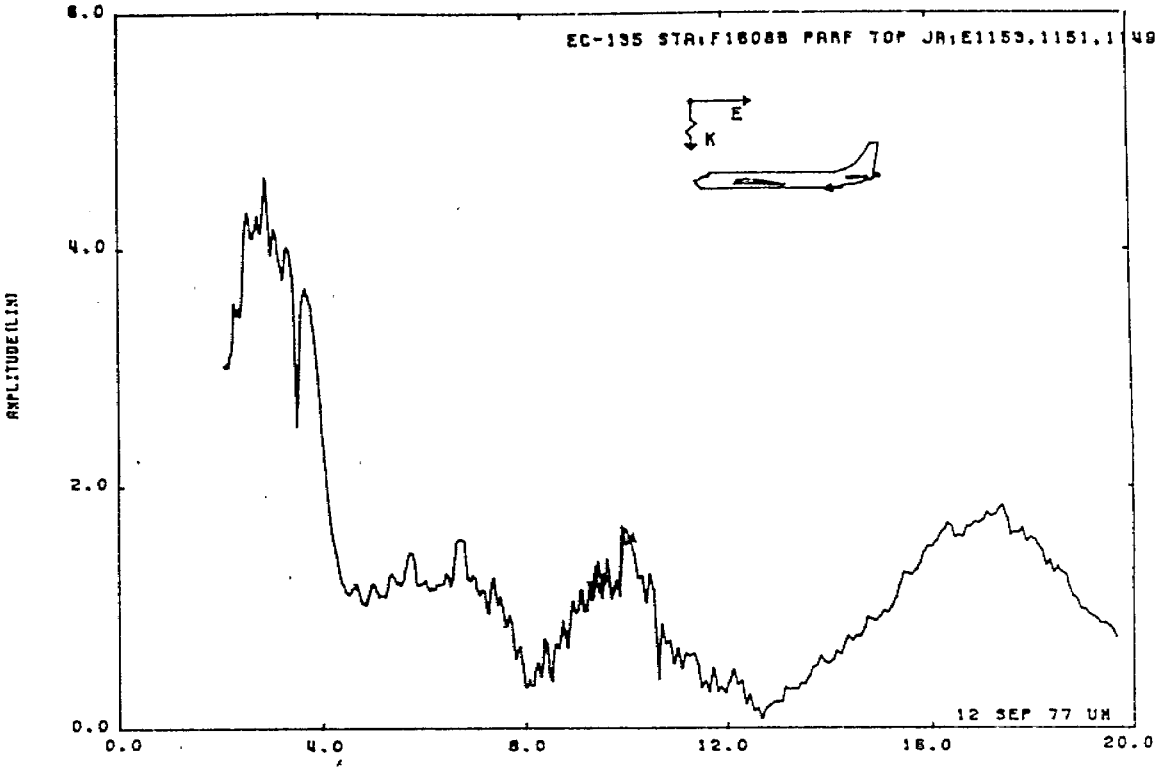

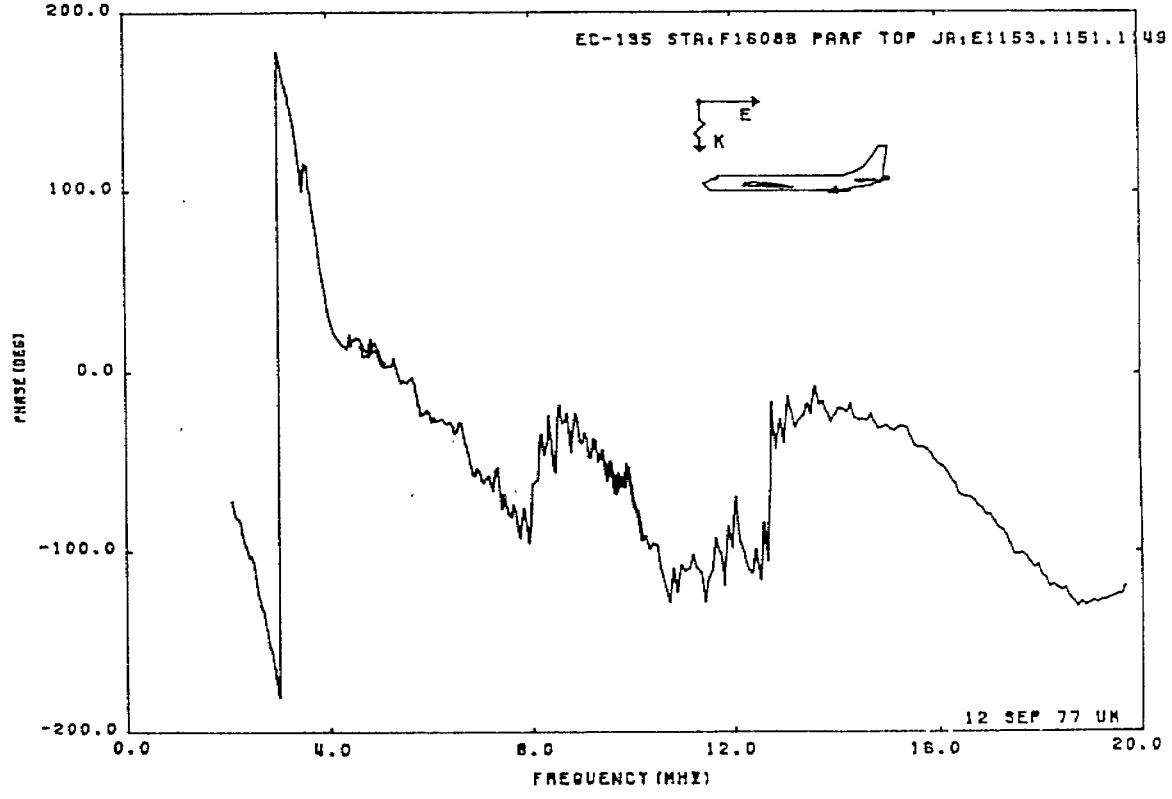

Figure 1: Raw data measured on EC-135 at STA:F1608B.

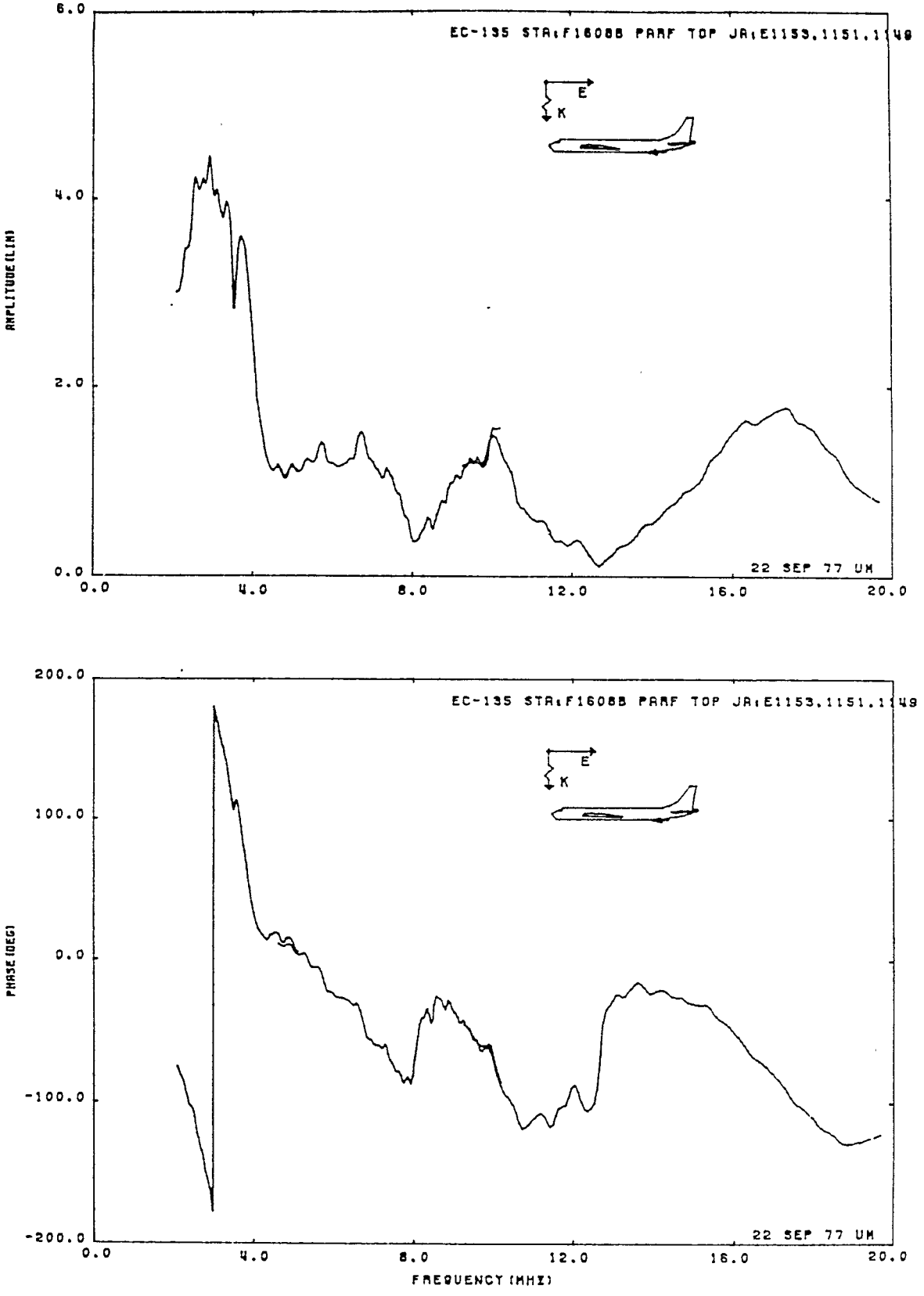

Figure 2: Data of Figure 1 filtered with f_c = 20 and n = 2.

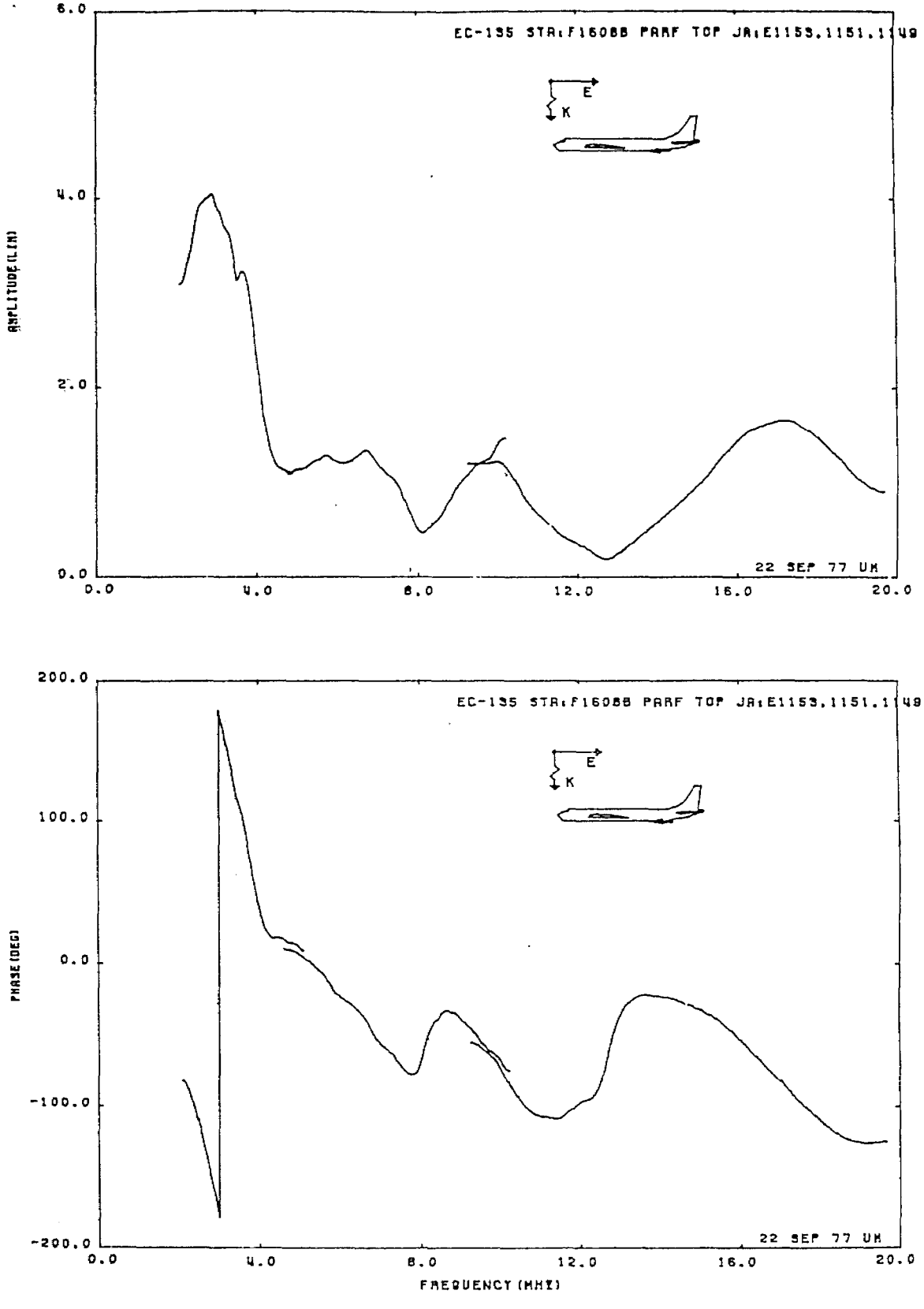

Figure 3: Data of Figure 1 filtered with $f_c = 5$ and $n = 2$.

3. MODEL-LEAD INTERACTION IN CHARGE MEASUREMENTS

The external shielded loops used to measure the current on small scale model aircraft in a simulated free space environment have been found adequate in most measurement situations [4]. When placed on a model, the loop itself is separated from the surface by the small (approximately 0.5 mm) thickness of the dielectric spacer. There is therefore no direct current path between the loop and the model, and the effect of any capacitative coupling is believed negligible for all practical purposes.

Charge probes, on the other hand, are rather different in design and the type that we have used most is a small monopole normal to the surface. The signal lead is passed through a slot cut in the surface and eventually leaves the model at some point on the other side. The coax in this case is electrically connected to the model using conducting tape; and if the point at which the coax leaves the model is improperly chosen, the lead can interact with the model and so distort the fields which are to be measured. Thus, a coax which

---

4. Valdis V. Liepa, "Sweep Frequency Surface Field Measurements," Sensor and Simulation Note 210, 1977.

leaves from the nose of an aircraft model will not distort the charge distribution when the excitation is antisymmetric, but with symmetric excitation (E parallel to the fuselage) where the dominant currents on the fuselage are axial, the conducting lead will provide a continuation of the current path and change completely the frequency response of the aircraft. In most measurement situations it is fairly easy to find a place on the model at which the coax can be taken from the surface with minimal distortion of the field being measured. In some cases the place can be located using a theoretical argument, and in others a combination of intuition and a few trial measurements has proved to be sufficient.

From a theoretical point of view a thin conducting lead attached to the model will not perturb the field, provided it is perpendicular to both the incident and scattered electric vectors. For a symmetric model such as an aircraft, the condition is met when the incident electric vector is perpendicular to the plane of symmetry (antisymmetric excitation) and the coaxial lead is in this plane. On the other hand, when the excitation is symmetric there is no universally valid prescription for positioning the lead and selecting the optimum location of the point at which the lead is taken from the surface, but in general it has been found most effective to choose the point on the shadow side close to the middle of the model. With aircraft such as the

EC-135, F-111 and E-4 (747) illuminated from the top, the best point is at the center of the bottom of the fuselage in line with the trailing edge of the wings.

From a single measurement made with the lead in a particular position, there is almost no way to estimate what effect the lead may have, particularly in the case of symmetric excitation. A procedure that could be used is to repeat the measurement using models of different scales at the corresponding laboratory frequencies, but this is not always feasible, and substantially increases the time and effort required to obtain the needed data. There is, however, an alternative approach in which the original measurement is repeated but with the lead departure point changed while still remaining in the general area where minimal interaction is expected. As an example, consider the measurement of the charge at STA:F1350T for topside incidence with the electric field parallel to the fuselage. In the first case the lead is taken from the bottom of the fuselage at the point in line with the trailing edge of the wing (see Figure 4 of [1] for a photograph of this situation), and the measurement is then repeated with the departure point moved a distance equal to 3/4 of the wingspan towards the nose. The measured data are shown in Figure 4. The two sets of data are almost identical; and though there is about 5 or 10 degrees change in phase around 9 MHz, the amplitudes are very small here so that even a small amount of noise has a noticeable effect.

The fact that changing the departure point of the lead produces no significant change in the measured data strongly suggests that any model-lead interaction that may exist has no effect on the field at the point where the measurement is made. If we regard the measured field as consisting of the vector sum of the true (undistorted) field and a model-lead perturbation, changing the lead configuration will modify the amplitude and phase of the undesired interfering signal, and thereby affect the net field in some manner, e.g., amplitude, phase,or change in null positions. The absence of any such effect is evidence that the interference is negligible, and that the measurements are not distorted by the conducting lead. On the other hand, if the measured data do change, it would appear that either or both sets of data have been affected by the lead; and it is then necessary to repeat the measurements with other positionings of the lead until the charges are reduced to an acceptable level.

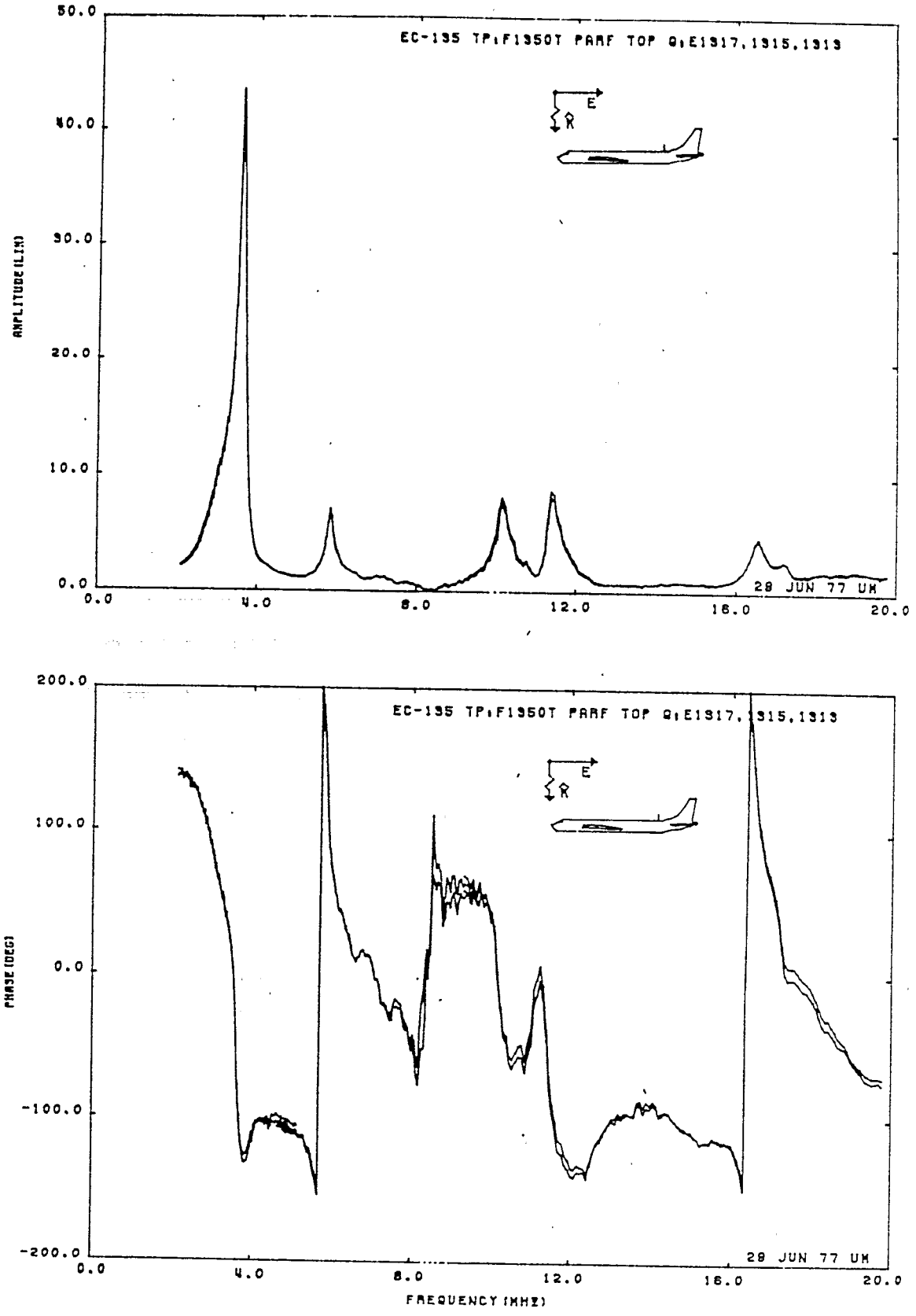

Figure 4: Charge measured at STA:F1350T for two signal lead configurations.

4. EFFECT OF HF WIRE ANTENNAS

The first measurements [5] made on the EC-135 model aircraft showed sharp (resonant) spikes in the current at STA:F1200T when HF wires were present; but since they were considered spurious and caused by probe-lead interactions, they were neglected in the manual reduction and plotting of the data. However, similar measurements made under the present program also showed the same type of behavior. The spikes occur not only in the current data but in the charge data as well, and after numerous tests and trial measurements it has been concluded that they are real and caused by the resonances of the HF wire antennas. The resonances are most pronounced in measurements made under the wires at STA:F1350T for topside incidence with the electric field parallel to the fuselage.

To better understand the effect of HF wires, the charge was measured at STA:F1350T in the four cases (a) with no wires, (b) with a single shorted wire only, (c) with a single open wire, and (d) with both wires present. Charge was chosen in preference to the current because the charge probe is smaller and, being brought out from within the model, is less likely to be affected by probe-model interaction.

---

5. Valdis V. Liepa, "Surface Field Measurements on Scale Model EC-135 Aircraft," Interaction Application Memo 15, 1977.

The amplitude data are presented in Figures 5 through 7. Figure 5 shows the charges with and without the two HF wires. The wires have a considerable effect and increase the amplitude from 5 to 50 at 3.5 MHz, as well as producing smaller peaks at other frequencies. The case of a single shorted wire is shown in Figure 6 and here the resonances are fewer and smaller though still clearly evident. The frequencies at which they occur correspond to wire lengths of 0.5, 1.0, and 1.5 wavelengths, as expected on the basis of a transmission line shorted at both ends. With the open wire (see Figure 7), however, the resonant frequencies are shifted and now correspond to wires 0.25 and 0.75 wavelength long. The resonances are those of a transmission line shorted at one end but open at the other. The peaks are about three times larger than for the shorted wire, and this is again consistent with a transmission line model where the electric field or charge has a maximum near the open end and a minimum at the short.

If the charge amplitudes of Figures 6 and 7 are added the resulting curve is similar to that of Figure 5 except in the immediate vicinity of 3.5 MHz, where the charge in Figure 5 is larger than the sum of the charges for the individual wires by about a factor 2. This is not surprising since when two wires are present most of the energy is supported by them, rather than by a wire and the fuselage as in the other cases. The factor 2 is then consistent with the higher Q of a thin scatterer or radiator.

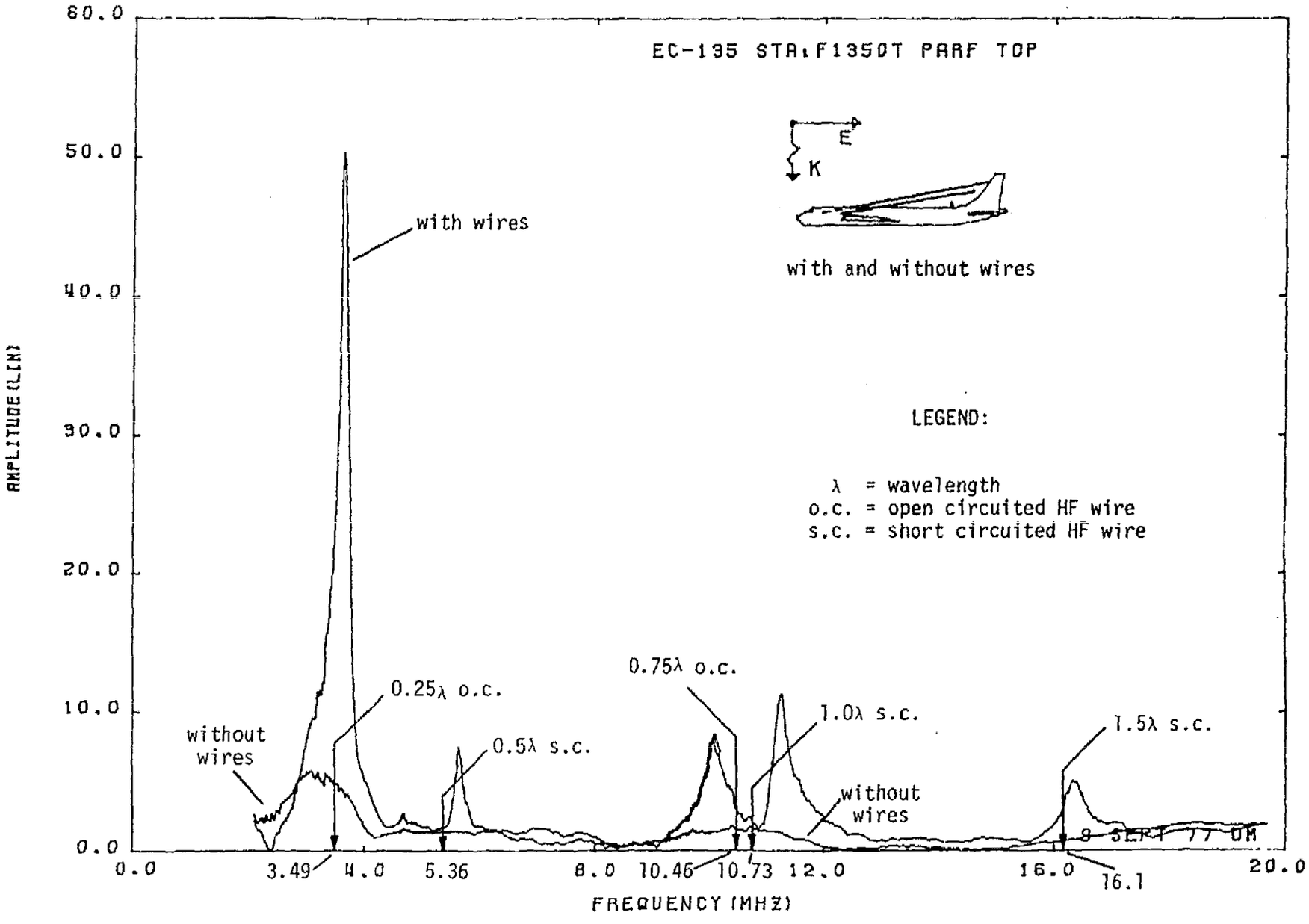

Figure 5: Charge amplitude at STA:F1350T with and without HF wires.

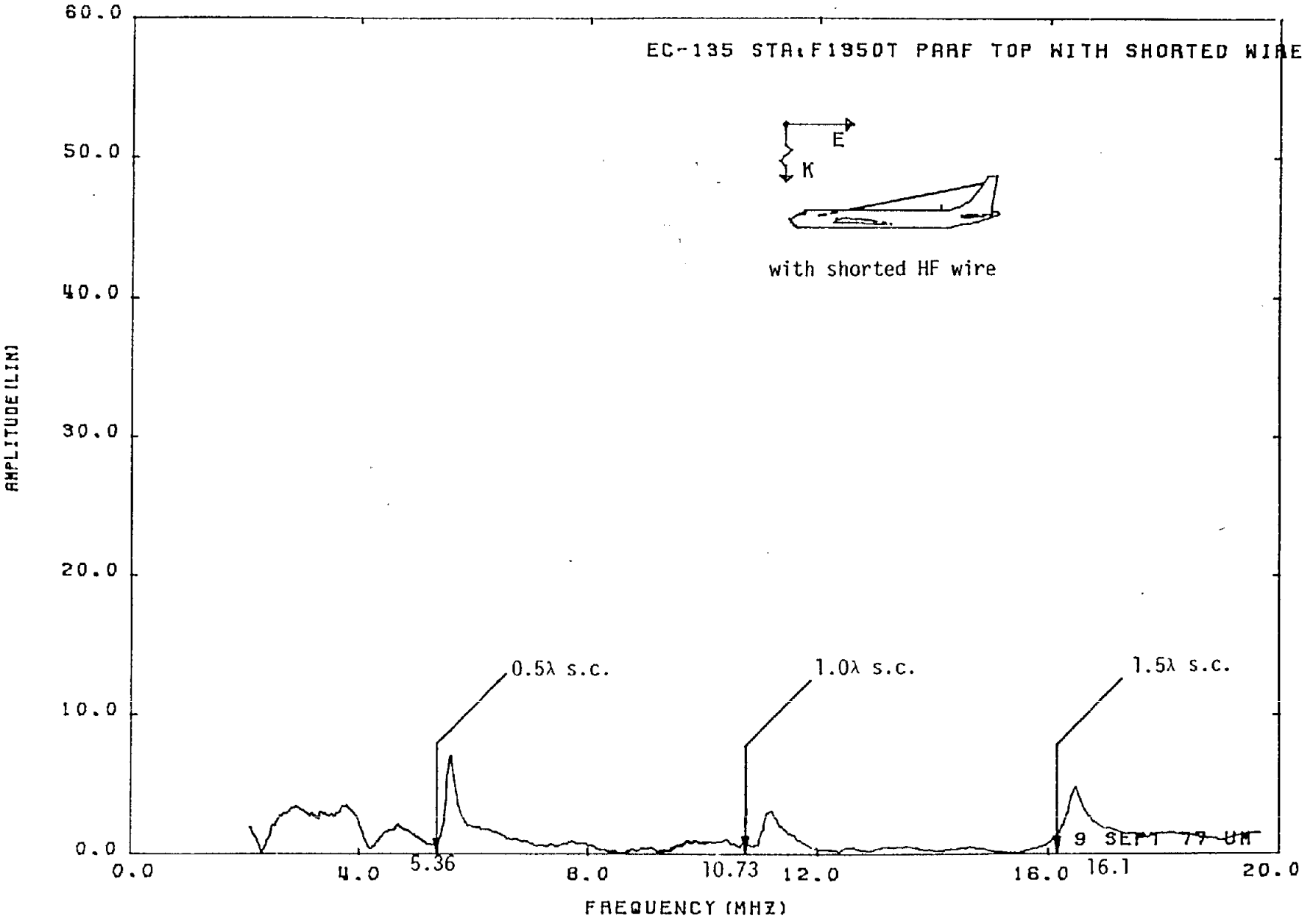

Figure 6: Charge amplitude at STA:F1350T with shorted HF wire.

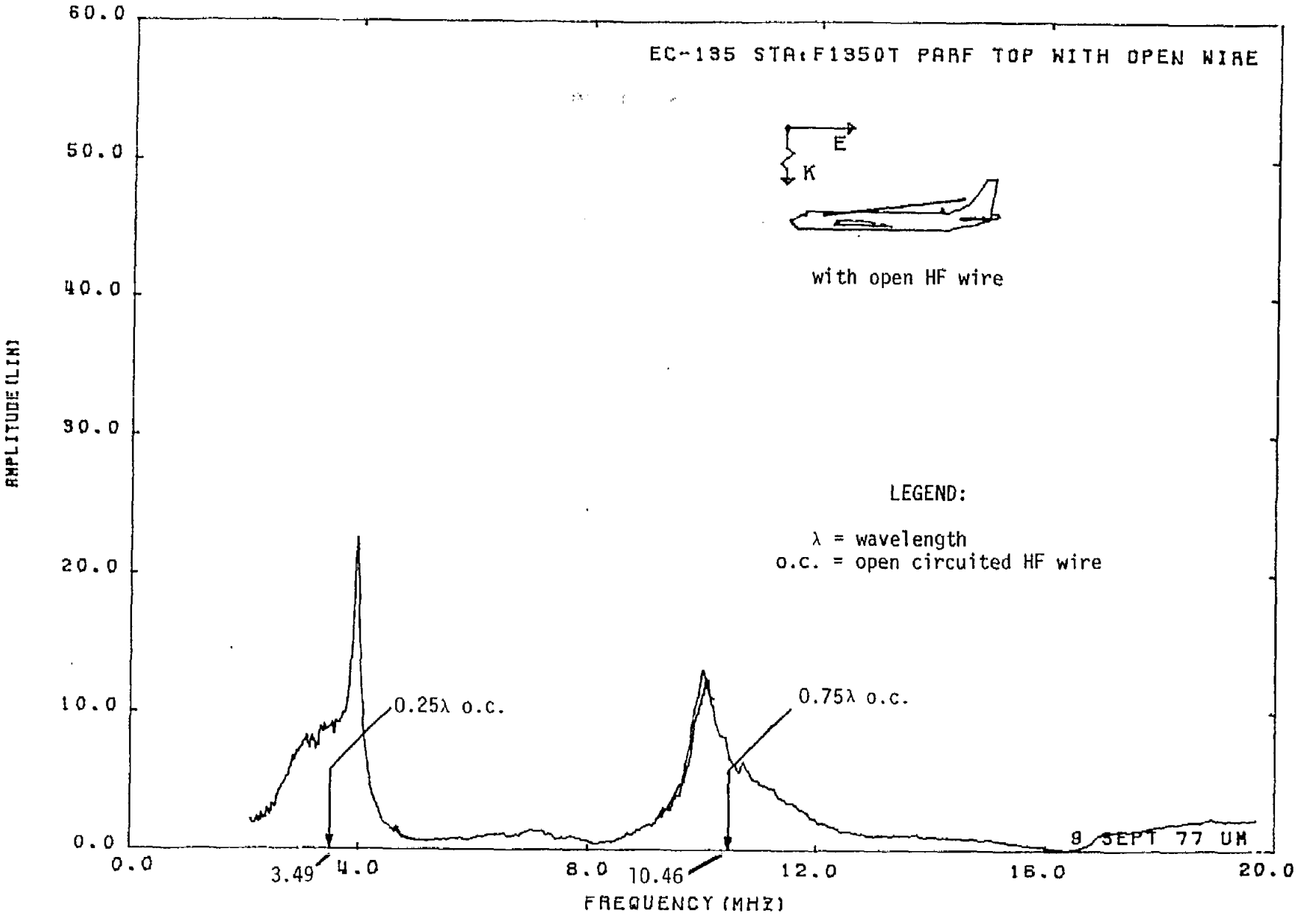

Figure 7: Charge amplitude at STA:F1350T with open HF wire.

5. SURFACE FIELD PHASE AT THE REAR OF CYLINDRICAL-LIKE OBJECTS

To resolve a controversy about the phase behavior of the surface field at the rear of cylinders and cylindrical-like bodies such as an airplane fuselage, the surface fields were measured on a number of metallic cylinders with open and closed ends.

The models used were three hollow steel pipes whose diameters and lengths (in inches) were 0.715 and 8.46, 1.735 and 16.88, and 1.165 and 54.88. All three were fitted with copper caps which were soldered in place to produce closed squared-off ends, but the second pipe measurements were first made with the ends of the cylinder open to examine the effect of the termination. As simulators of the fuselage of the EC-135 aircraft whose "average" diameter at station F520 is 155 inches, the three pipes have scale factors 1/216.78, 1/89.34, and 1/133.05 respectively based on their diameters, and the measured data obtained will be shown for full scale pipes at the full scale frequencies derived using these scale factors. Details of the cylinders and their dimensions are given in Table 1.

TABLE 1

CYLINDER DESCRIPTION

No.	Type	Physical Size			Scaled Size*		
		Length (cm)	Diameter (cm)	L/D	Length (cm)	Diameter (cm)	Scaling Factor
1	closed	21.48	1.82	11.827	4656.	393.7	216.78
2a	closed	42.94	4.41	9.736	3836.	393.7	89.34
2b	open	42.84	4.41	9.724	3827.	393.7	89.34
3	closed	139.38	2.96	47.105	18544.	393.7	133.05

*Values scaled to the average fuselage diameter of EC-135 at STA:F520.

The cylinders were mounted horizontally and illuminated with a field incident in a plane perpendicular to the generators with the incident electric field horizontal. Using a small current loop probe the horizontal component of the current was measured at the center front of each cylinder and the corresponding point at the back. In addition, for cylinder numbers 1,

2a and 2b, the currents were also measured at the front and back at points 1/4 of the length from an end. Calibration was with respect to the incident field at the front in all cases. The measurements made are listed in Table 2 and the data are presented in Appendix B. Here we present only the data relevant to this section.

TABLE 2

MEASUREMENTS PERFORMED

(The data are in Appendix B)

Cylinder Number	Front Center	Back Center	Front 1/4*	Back 1/4
1	Figure B.1	Figure B.2	Figure B.3	Figure B.4
2a	B.5	B.6	B.7	B.8
2b	B.9	B.10	B.11	B.12
3	B.13	B.14		

*The Front 1/4 and Back 1/4 indicates the measurement made at a point 1/4 of the length from an end.

From corresponding measurements on the open and closed cylinders it is at once evident that open ends have no significant effect on the currents at the stations considered. Thus, for example, the phase curves in Figures B.6b and B.10b (Appendix B) are virtually identical. It is therefore sufficient to confine attention to the closed cylinder data.

To elucidate the manner in which the current on the rear of a cylinder is excited, consider for example the measurements made at the center of the second cylinder with the ends closed: Figures 8a, b and 9a, b. At the front the phase is almost constant for f > 12 MHz and oscillates about the zero value given by physical optics. At the rear, however, the phase shows a progressive decrease (time convention $e^{i\omega t}$) with increasing frequency, and the mean rate of decrease of approximately 26.2°/MHz implies an effective phase center about 2182 cm behind the cylinder, i.e., an excitation path of this length. The only way that it is possible is if the dominant excitation is around the ends rather than over the (half) circumference.

For excitation across the ends and hence along the rear of the cylinder to the center of the back, the path length is D + L/2, and assuming that the phase velocity is that of light the progressive phase in degrees is

$$\phi = \frac{-360\ f_{MHz}(D + L/2)_{cm}}{c} + 180$$

where c is the velocity of light in cm/sec and the 180 degree phase change has been added to have the current in the same direction as that in front of the cylinder. For the second cylinder,

$$\phi = -27.760\ f_{MHz} + 180$$

and when this phase is subtracted from the measured phase, the phase at the rear of the cylinder is shown in Figure 10. The progressive phase variation has now been eliminated, and the slight overcorrection or rise in the phase curve with frequency that now exists could be attributed to the approximate nature of the above formula and/or measurement error caused by slight alignment errors in positioning the cylinder parallel to the incident electric vector.

A similar analysis can be applied to the phase data at the rear of the other cylinders measured, and leaves no doubt that for cylinders of the electric lengths considered the primary means of excitation of the rear is via the ends. It now follows that computed data for an infinite cylinder have little bearing on the interpretation and understanding of the surface fields on the rear of a finite cylinder. This is in contrast to the situation for points on the front.

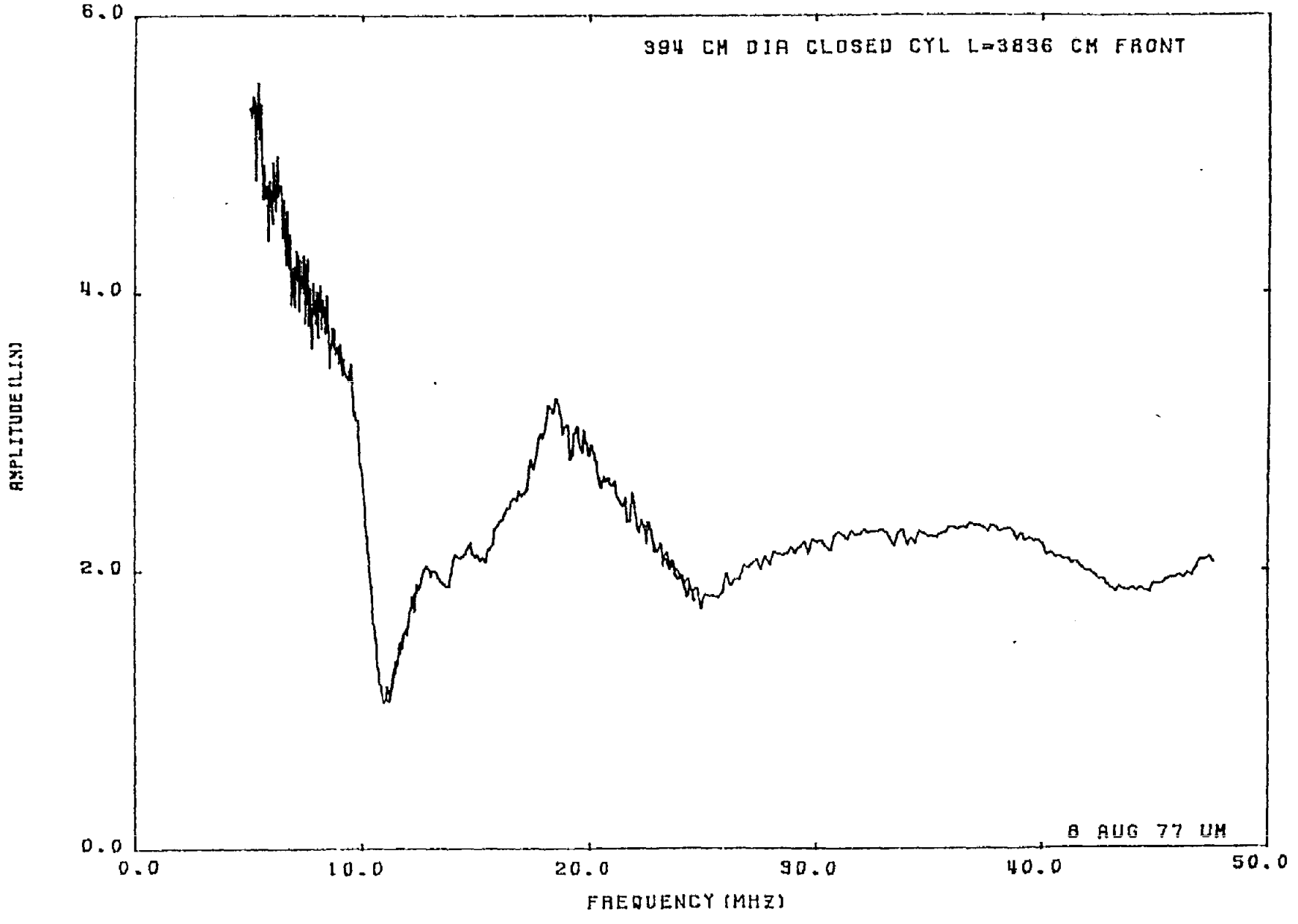

Figure 8a: Current amplitude at front center of cylinder No. 2a.

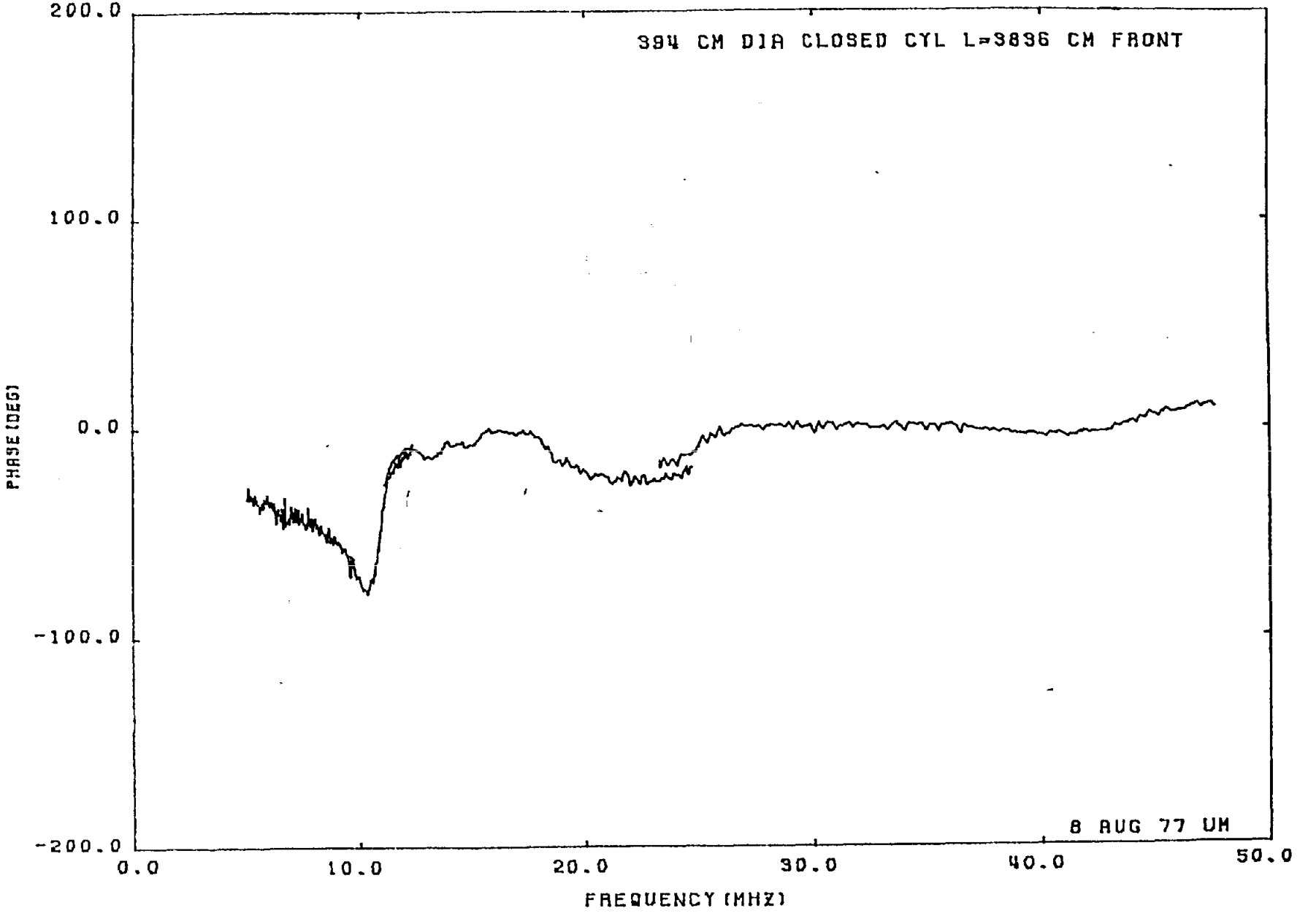

Figure 8b: Current phase at front center of cylinder No. 2a.

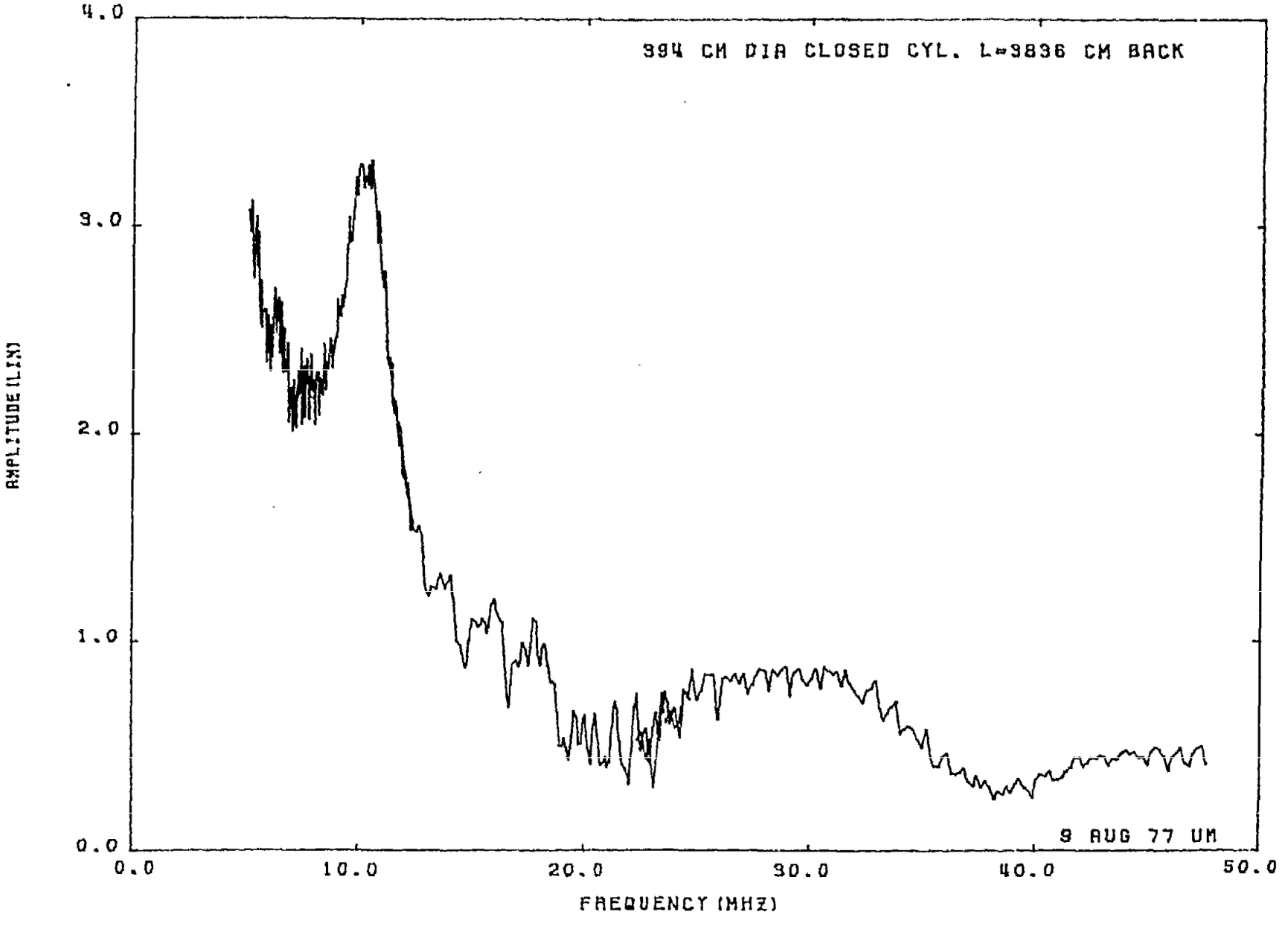

Figure 9a: Current amplitude at back center of cylinder No. 2a.

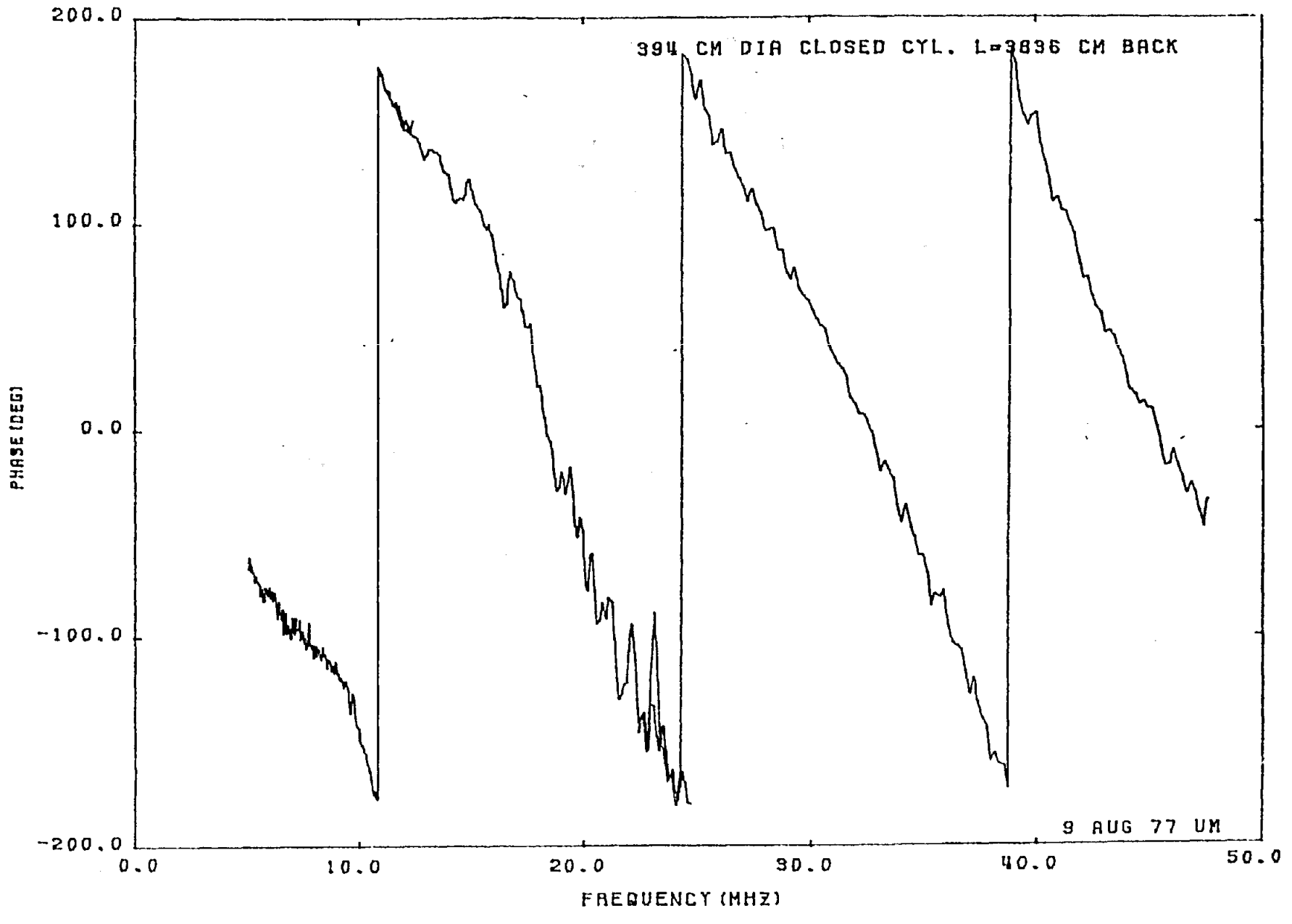

Figure 9b: Current phase at back center of cylinder No. 2a.

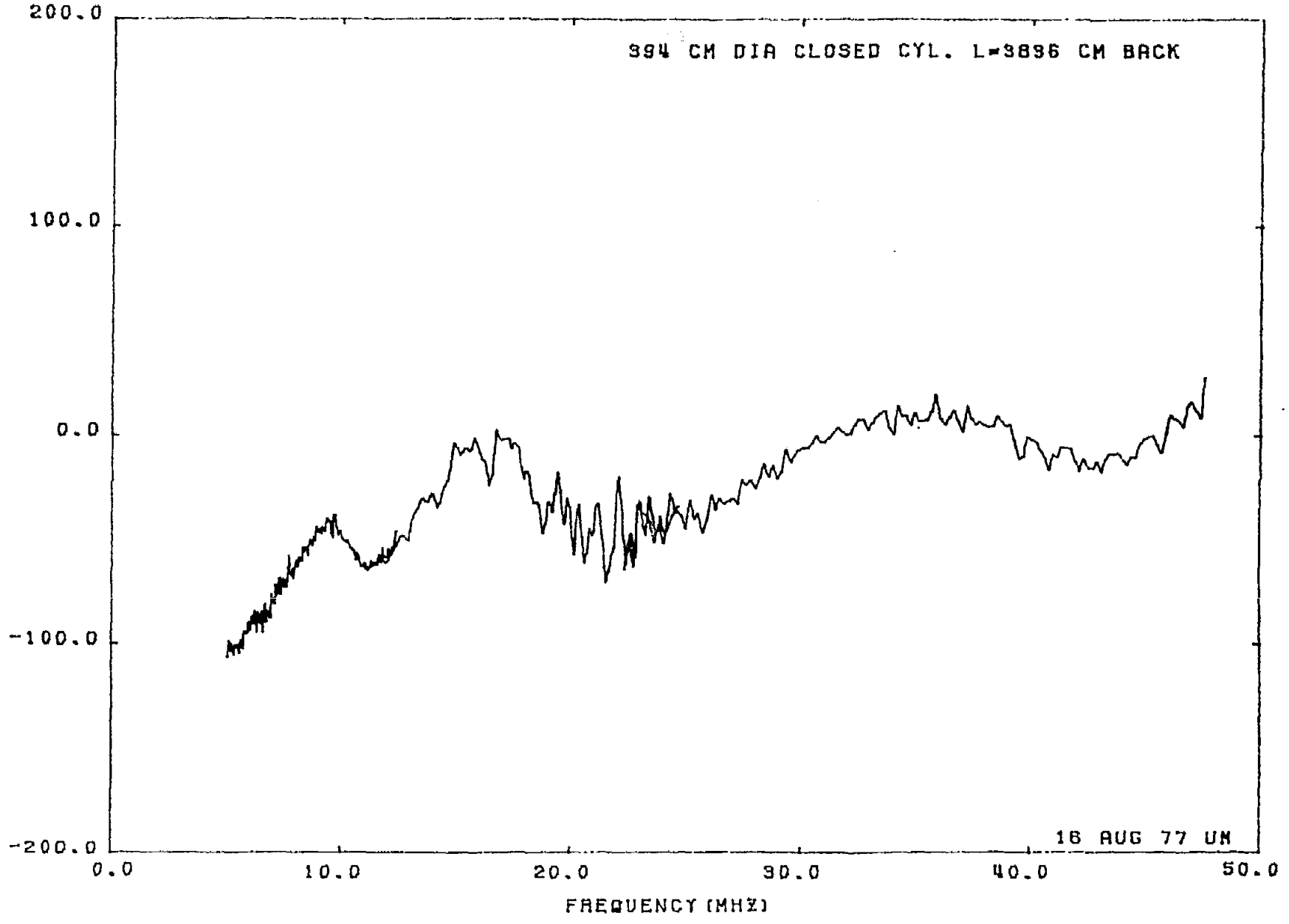

Figure 10: Phase in the back of the No. 2a cylinder after path length D + L/2 has been subtracted. (Compare with Figure 9b).

APPENDIX A

DISCRETE DATA FILTER PROGRAM

(For discussion see Section 2)

```
      COMPLEX B(3),A(138)
      DIMENSION F(138),AMP(138),PI(138),FILEN1(4)
      DIMENSION FILEN(4),COMNT1(18),COMNT2(18),TITLE(18)
      LOGICAL*1 FILE(30),BLANK
      INTEGER*2 LEN
      DATA BLANK/' '/
C
C  READING FROM THE ORIGINAL FILE
C
  110 WRITE(6,101)
  101 FORMAT(///,'ENTER FILE NAME')
      CALL SCARDS(FILE,LEN,0,LINNUM,&110)
      FILE(LEN+1)=BLANK
      CALL GTFILE(1,FILE,IFDUB,&120)
      GO TO 121
  120 WRITE(6,400)
  400 FORMAT('FILE DOES NOT EXIST')
      GO TO 110
  121 READ(1,34) FILEN1
  300 FORMAT(18A4)
      READ(1,300) COMNT1
      READ(1,300)COMNT2
      READ(1,300)TITLE
      READ(1,200)FMI,FMA,AMIN,AMAX,PMIN,PMAX,NN2
  200 FORMAT(4F8.3,2F8.2,I5)
      L2=MOD(NN2,3)
      LJ=NN2-L2-2
      READ(1,201)(F(J),AMP(J),PI(J),F(J+1),AMP(J+1),PI(J+1),F(J+2),
     *AMP(J+2),PI(J+2),J=1,LJ,3)
  201 FORMAT(3(2F8.3,F8.2))
      L3=3-L2
      GO TO (31,32,33),L3
   31 READ(1,202)F(NN2-1),AMP(NN2-1),PI(NN2-1),F(NN2),AMP(NN2),PI(NN2)
  202 FORMAT(2(2F8.3,F8.2))
      GO TO 33
   32 READ(1,203)F(NN2),AMP(NN2),PI(NN2)
  203 FORMAT(2F8.3,F8.2)
C
C  CONVERSION OF DATA INTO COMPLEX FORM
C
   33 DO 12 I=1,NN2
      PJ=PI(I)/57.2958
      A(I)=CMPLX(COS(PJ),SIN(PJ))*AMP(I)
   12 CONTINUE
```

```
45      C
46      C  FILTERING ROUTINE
47      C
48            WRITE(6,100)
49          100 FORMAT(/,'ENTER FILTER ORDER & CUTOFF FREQUENCY (CYCLES PER PLOT),
50             *IN FORMAT I2,G5.1')
51            READ(5,102)N,FC
52          102 FORMAT(I2,G5.1)
53            W=6.2832*FC
54            P=FLOAT(NN2)
55            T=1./P
56            XN=N
57            U=2.**(1./XN)*(1.+COS(W*T))-2.
58            V=U+2.-2.*COS(W*T)
59            Q=1./U*(V-SQRT(V**2-U**2))
60            B(1)=A(11)
61            DO 11 I=1,10
62            J=11-I
63            B(2)=(1.-Q)/2.*(A(J)+A(J+1))+Q*B(1)
64            B(1)=B(2)
65          11 CONTINUE
66            DO 10 K=1,N
67            B(3)=B(1)
68            DO 13 I=1,NN2
69            B(2)=(1.-Q)/2.*(A(I)+B(3))+Q*B(1)
70            B(1)=B(2)
71            B(3)=A(I)
72            A(I)=B(2)
73          13 CONTINUE
74            B(3)=B(1)
75            DO 10 I=1,NN2
76            J=NN2+1-I
77            B(2)=(1.-Q)/2.*(A(J)+B(3))+Q*B(1)
78            B(1)=B(2)
79            B(3)=A(J)
80            A(J)=B(2)
81          10 CONTINUE
82            DO 14 I=1,NN2
83            XR=REAL(A(I))
84            XI=AIMAG(A(I))
85            PI(I)=ATAN2(XI,XR)*57.2958
86            AMP(I)=CABS(A(I))
87          14 CONTINUE
88      C
89      C  CALCULATION OF THE NEW MINIMA & MAXIMA
90      C
91            AMIN=AMP(1)
92            AMAX=AMIN
93            PMIN=PI(1)
94            PMAX=PMIN
95            DO 15 J=2,NN2
96            IF(AMP(J).GE.AMIN)GO TO 16
97            AMIN=AMP(J)
98            GO TO 17
99          16 IF(AMP(J).LE.AMAX)GO TO 17
100           AMAX=AMP(J)
101         17 IF(PI(J).GE.PMIN)GO TO 18
```

```
102           PMIN=PI(J)
103           GO TO 15
104        18 IF(PI(J).LE.PMAX)GO TO 15
105           PMAX=PI(J)
106        15 CONTINUE
107     C
108     C  CREATION AND FILLING OF THE NEW FILTERED FILE .
109     C
110           WRITE(6,401)
111       401 FORMAT(/,'ENTER NAME FOR THE FILTERED FILE')
112           READ(5,34)FILEN
113           CALL CREATE(FILEN,0,0,0)
114           CALL SETDSN(8,FILEN)
115           WRITE(8,34)FILEN
116        34 FORMAT(4A4)
117           WRITE(8,300)COMNT1
118           WRITE(8,300)COMNT2
119           WRITE(8,300)TITLE
120           WRITE(8,501)FMI,FMA,AMIN,AMAX,PMIN,PMAX,NN2
121       501 FORMAT(4F8.3,2F8.2,I5)
122           L2=MOD(NN2,3)
123           LJ=NN2-L2-2
124           WRITE(8,502)(F(J),AMP(J),PI(J),F(J+1),AMP(J+1),PI(J+1)
125          *,F(J+2),AMP(J+2),PI(J+2),J=1,LJ,3)
126       502 FORMAT(3(2F8.3,F8.2))
127           L3=3-L2
128           GO TO(61,62,63),L3
129        61 WRITE(8,503)F(NN2-1),AMP(NN2-1),PI(NN2-1),F(NN2),
130          *AMP(NN2),PI(NN2)
131       503 FORMAT(2(2F8.3,F8.2))
132           GO TO 63
133        62 WRITE(8,504)F(NN2),AMP(NN2),PI(NN2)
134       504 FORMAT(2F8.3,F8.2)
135        63 GO TO 110
136           END
```

APPENDIX B

CURRENT DATA MEASURED ON VARIOUS CYLINDERS AS A FUNCTION OF FREQUENCY

(For discussion see Section 5, particularly Table 2, page 21.)

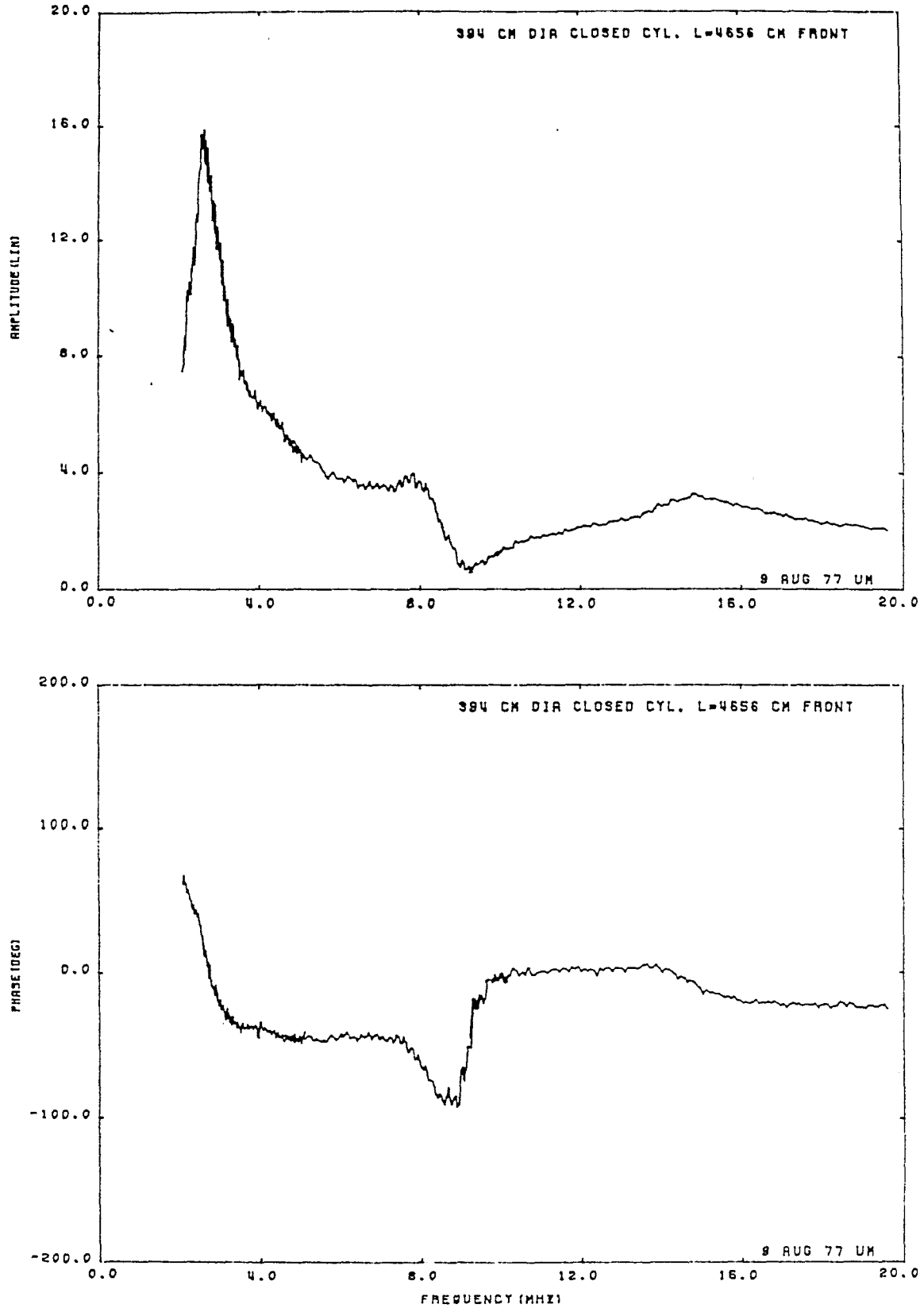

Figure B.1: Current at front center of cylinder No. 1.

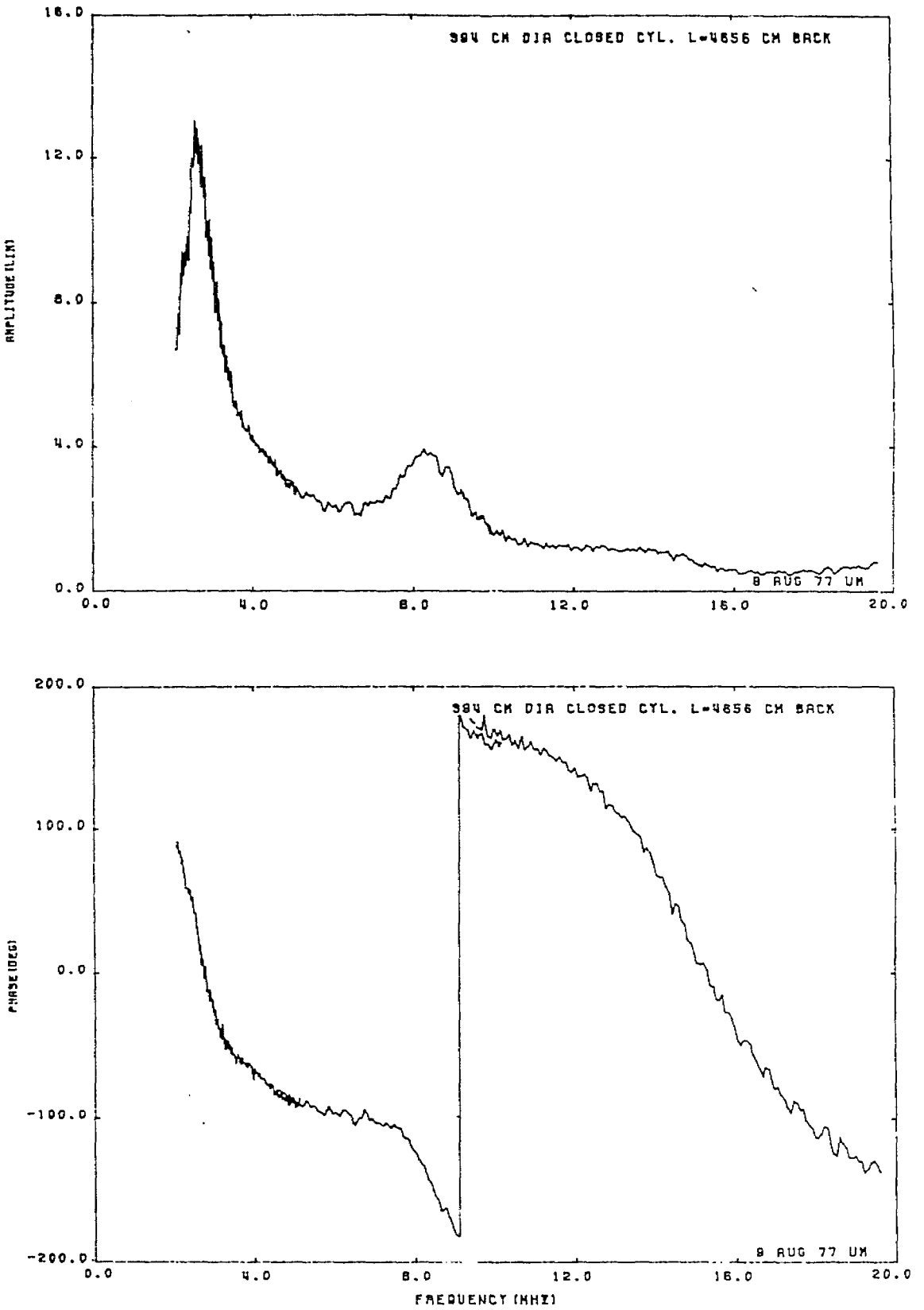

Figure B.2: Current at back center of cylinder No. 1.

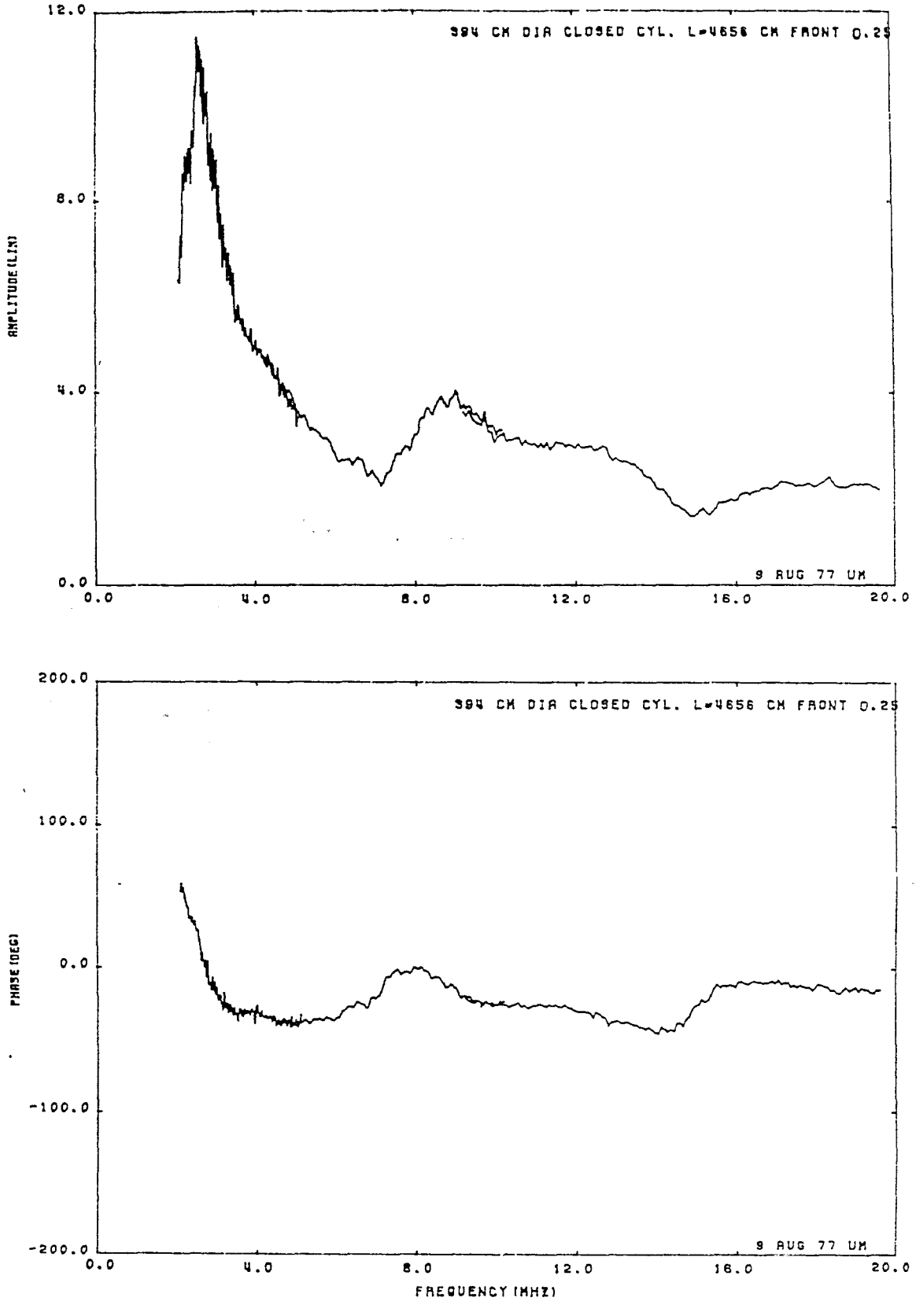

Figure B.3: Current at front 1/4 of cylinder No. 1.

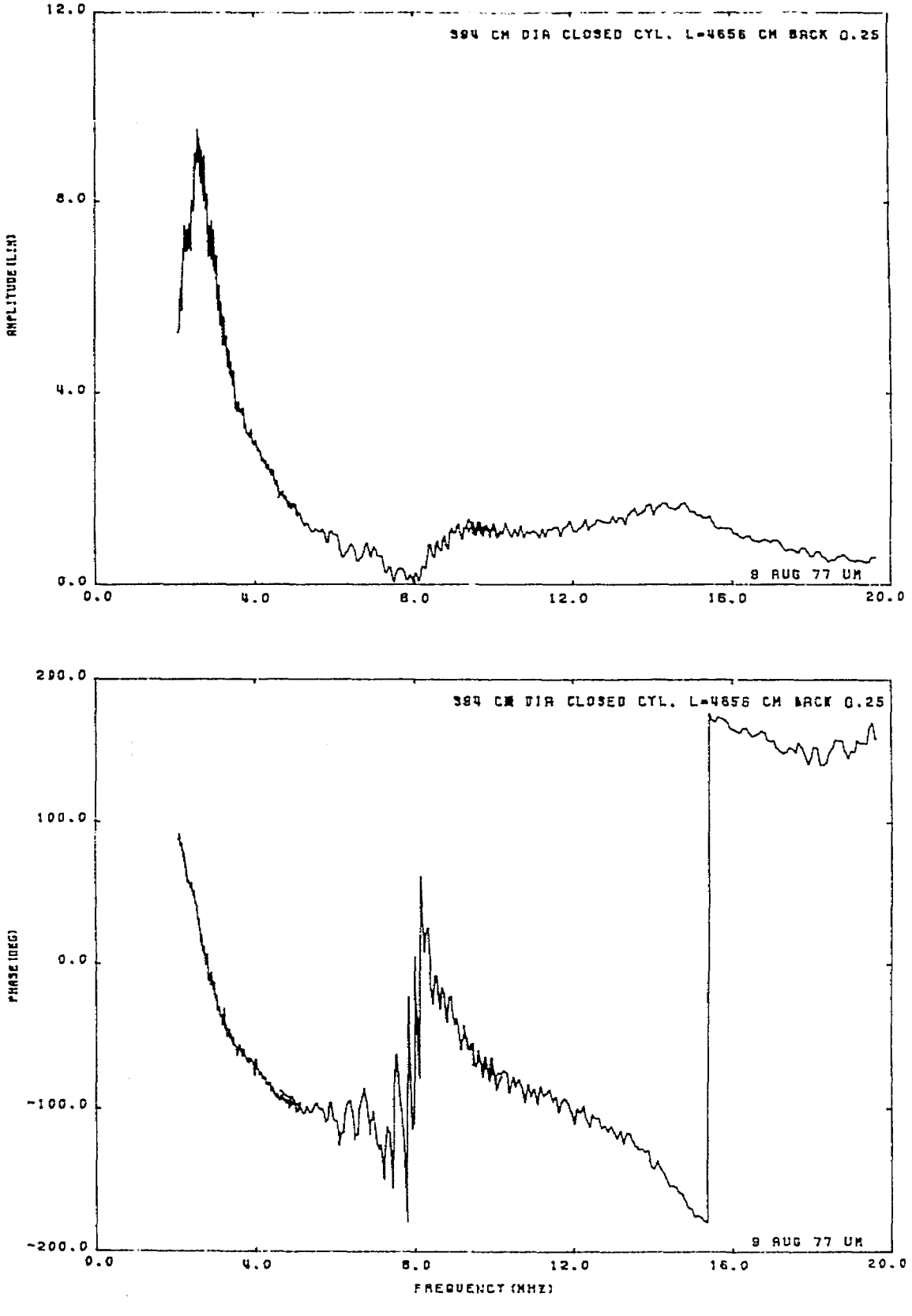

Figure B.4: Current at back 1/4 of cylinder No. 1.

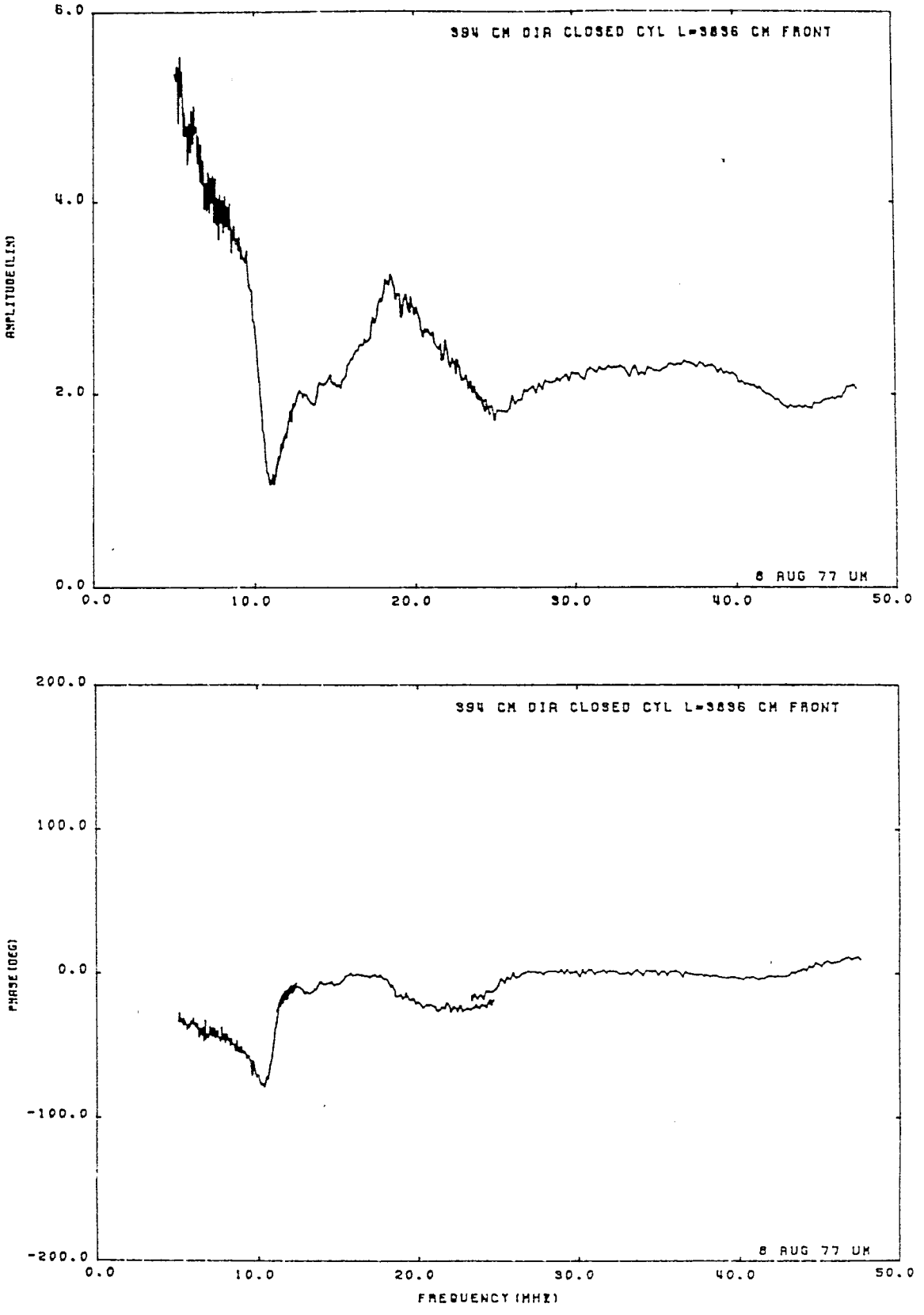

Figure B.5: Current at front center of cylinder No. 2a.

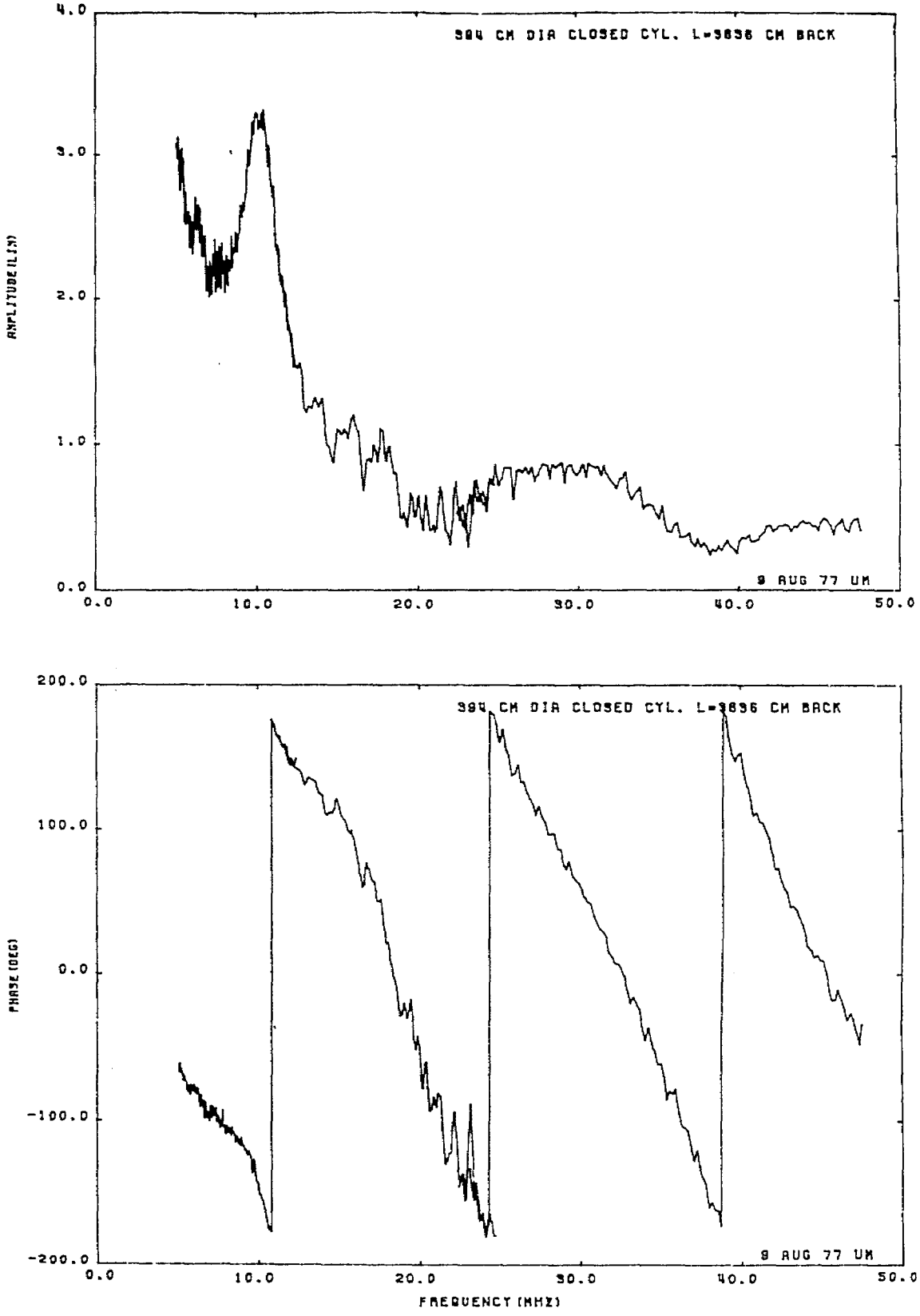

Figure B.6: Current at back center of cylinder No. 2a.

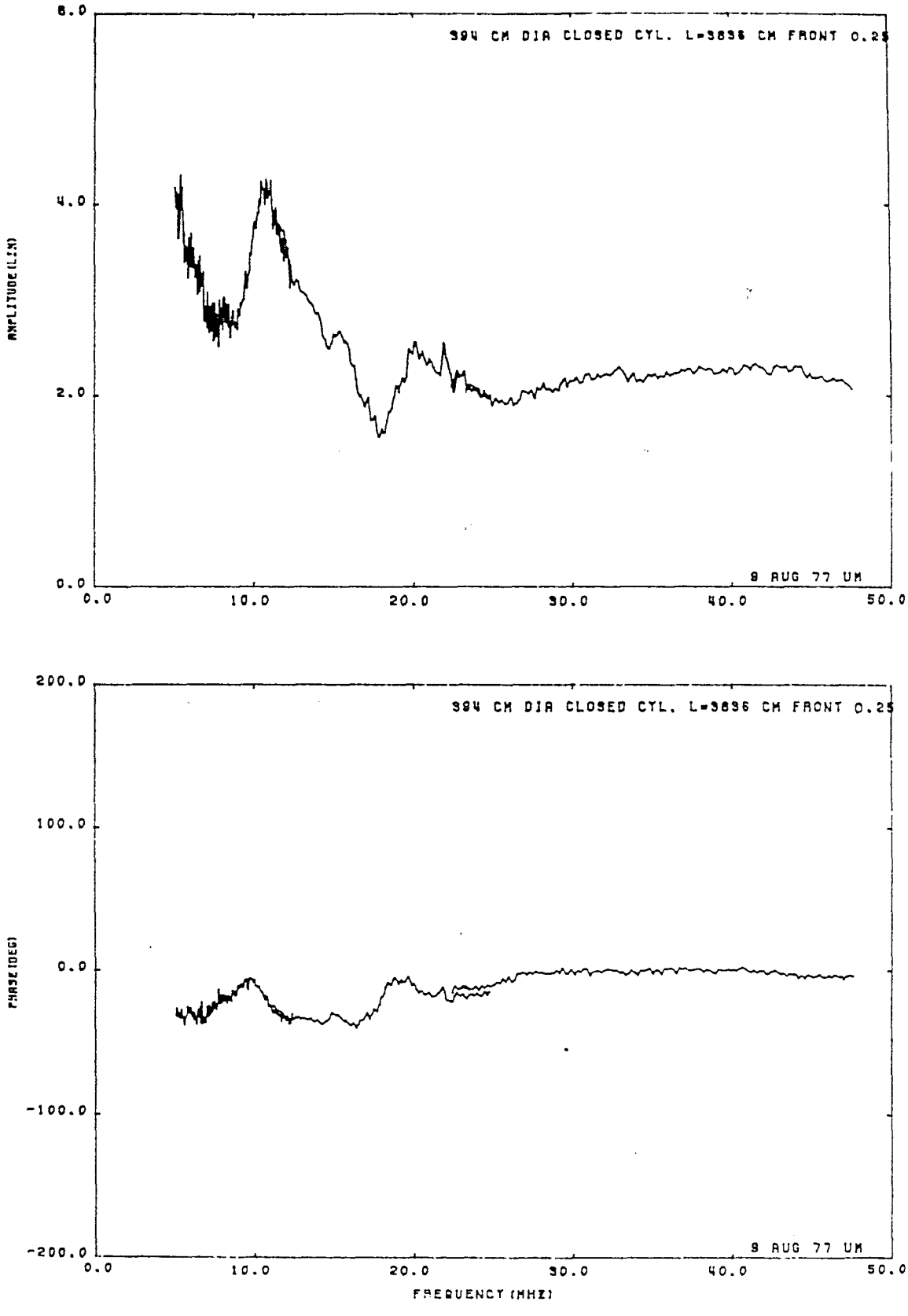

Figure B.7: Current at front 1/4 of cylinder No. 2a.

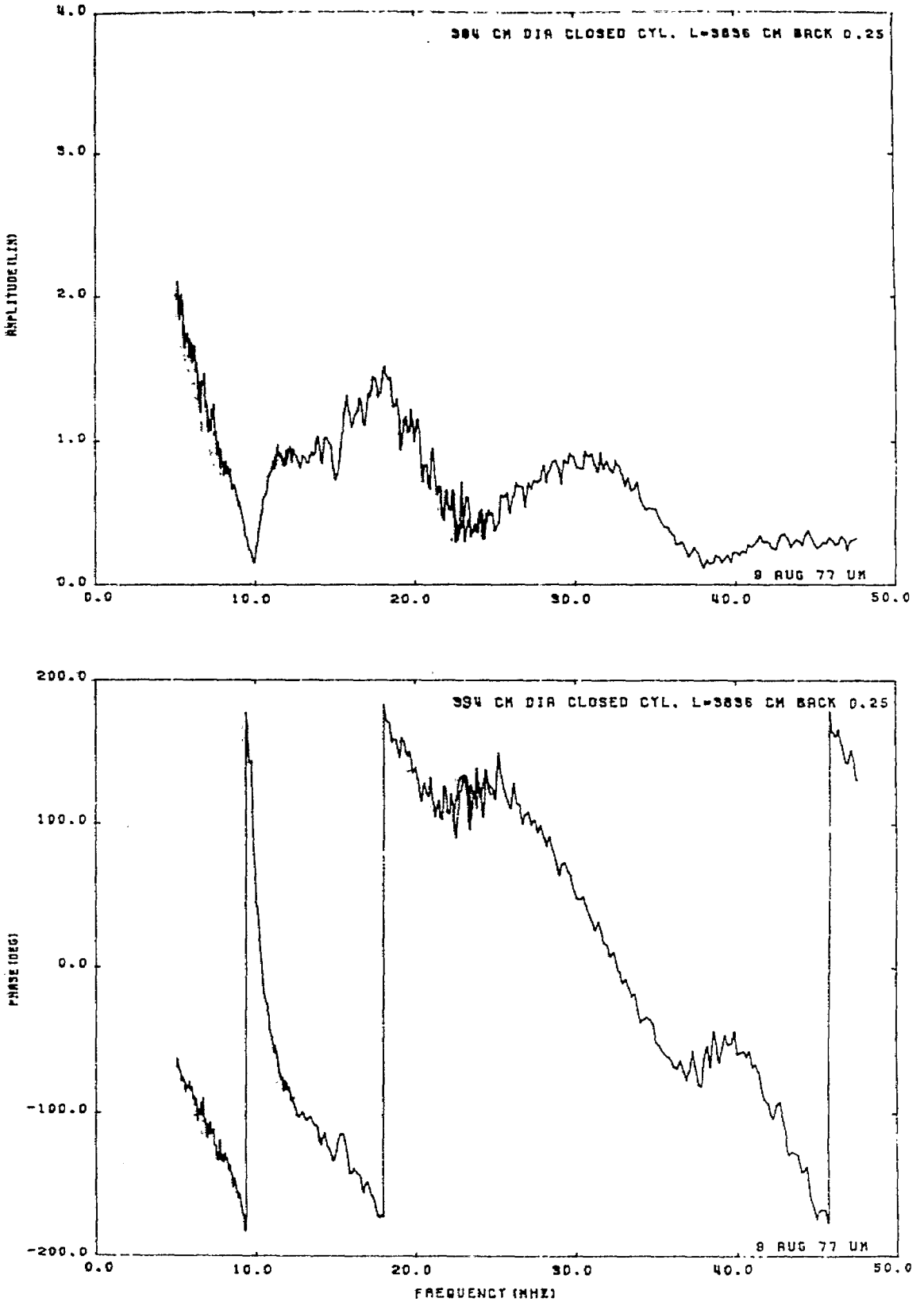

Figure B.8: Current at back 1/4 of cylinder No. 2a.

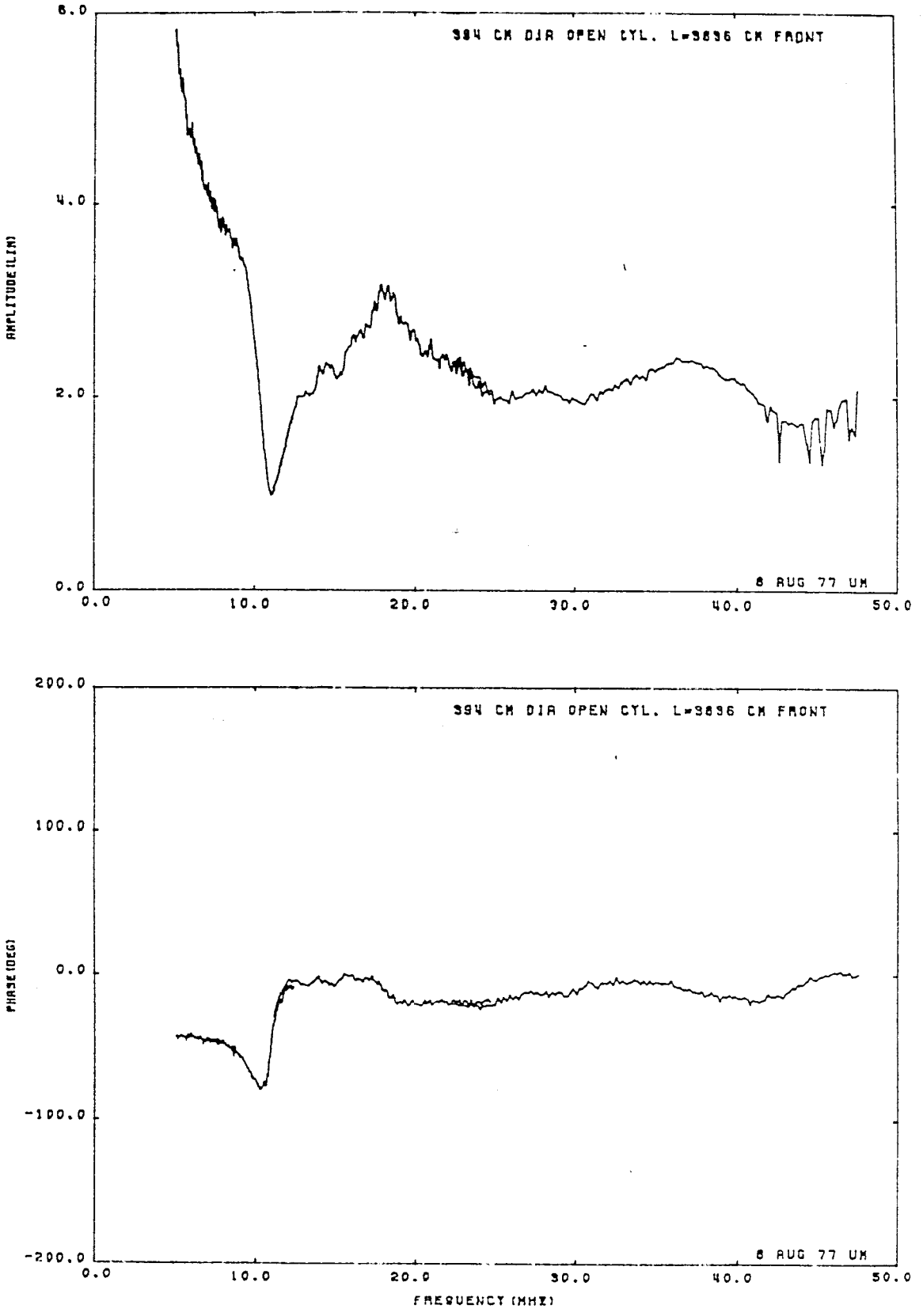

Figure B.9: Current at front center of cylinder No. 2b.

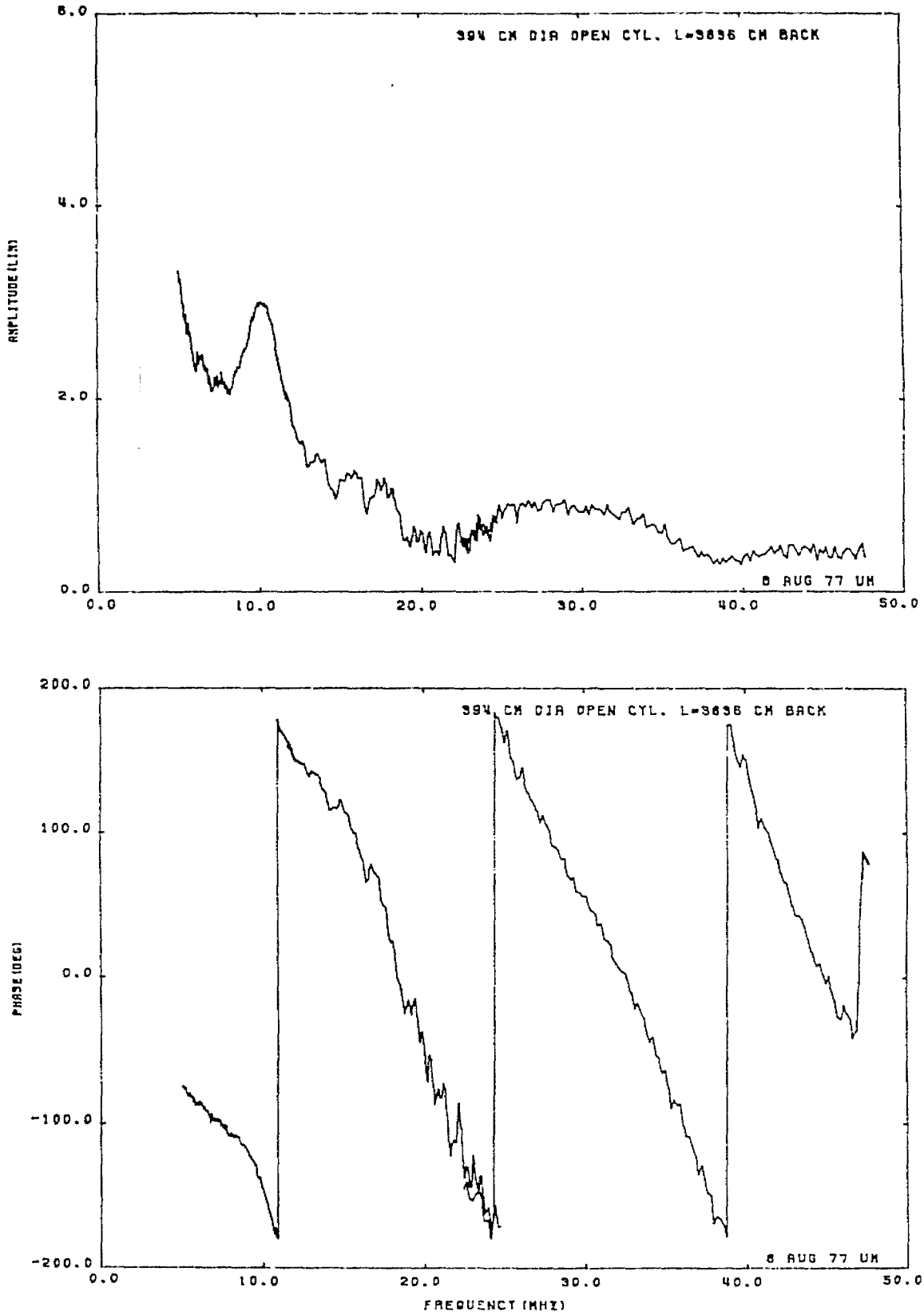

Figure B.10: Current at back center of cylinder No. 2b.

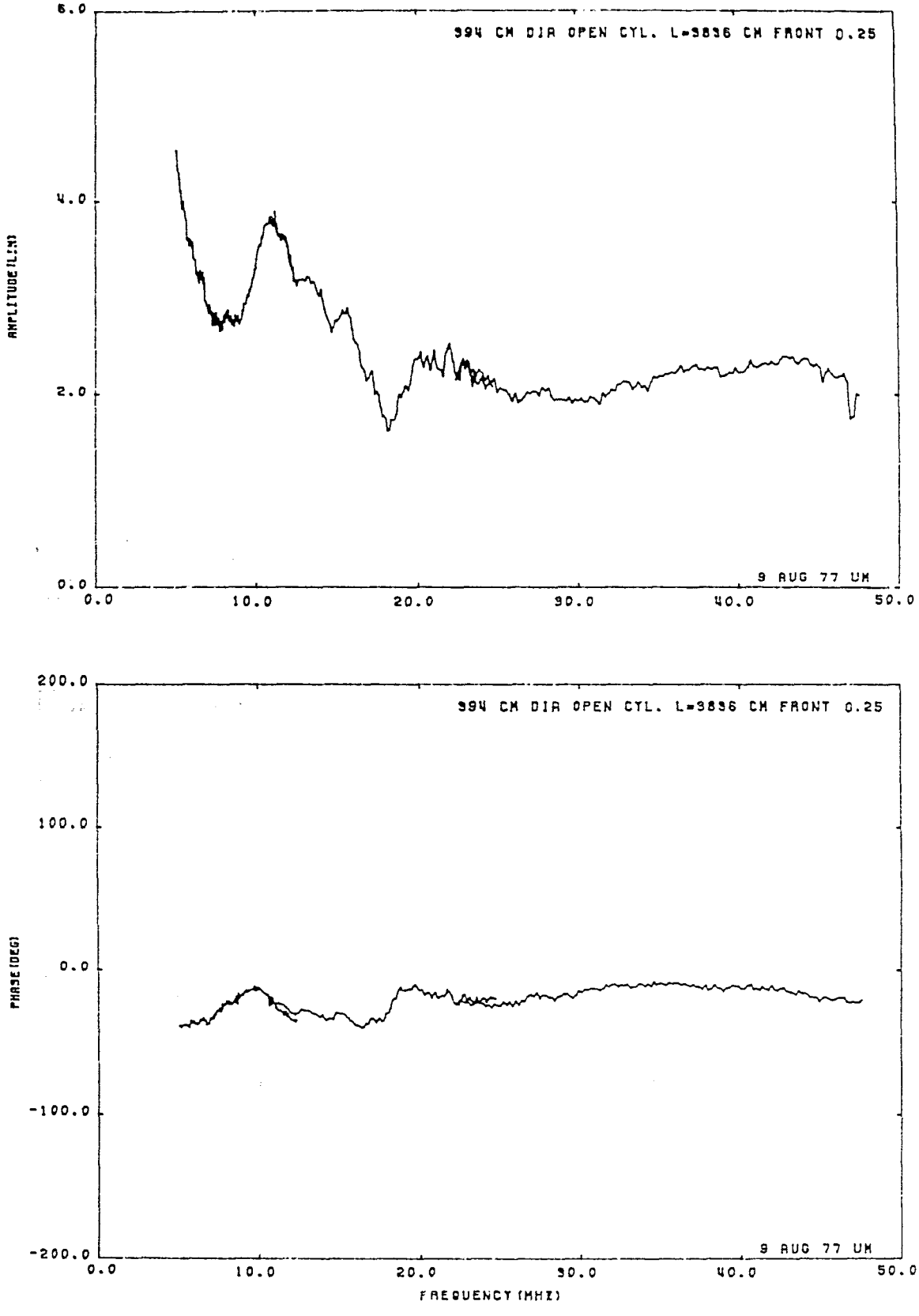

Figure B.11: Current at front 1/4 of cylinder No. 2b.

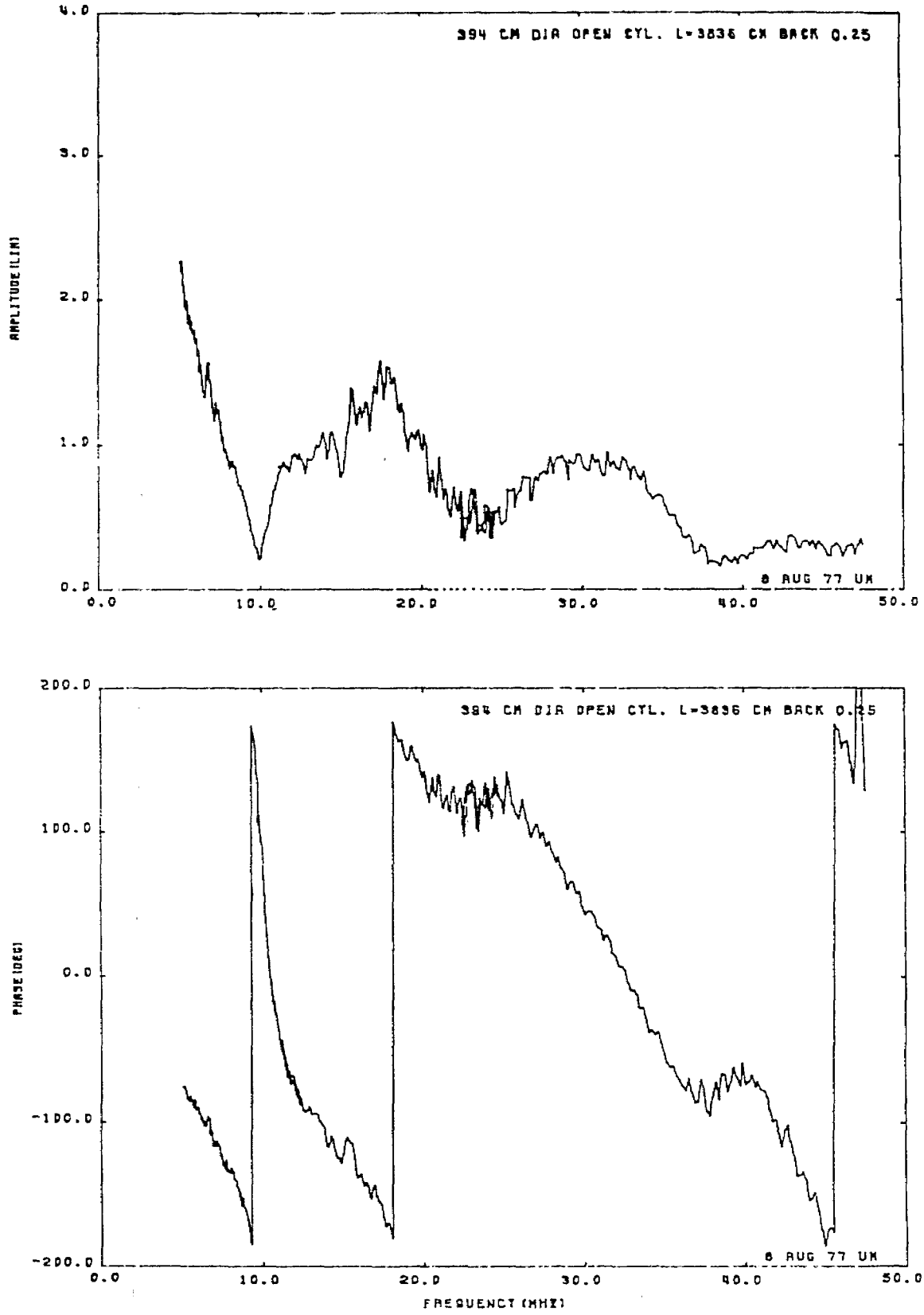

Figure B.12: Current at back 1/4 of cylinder No. 2b.

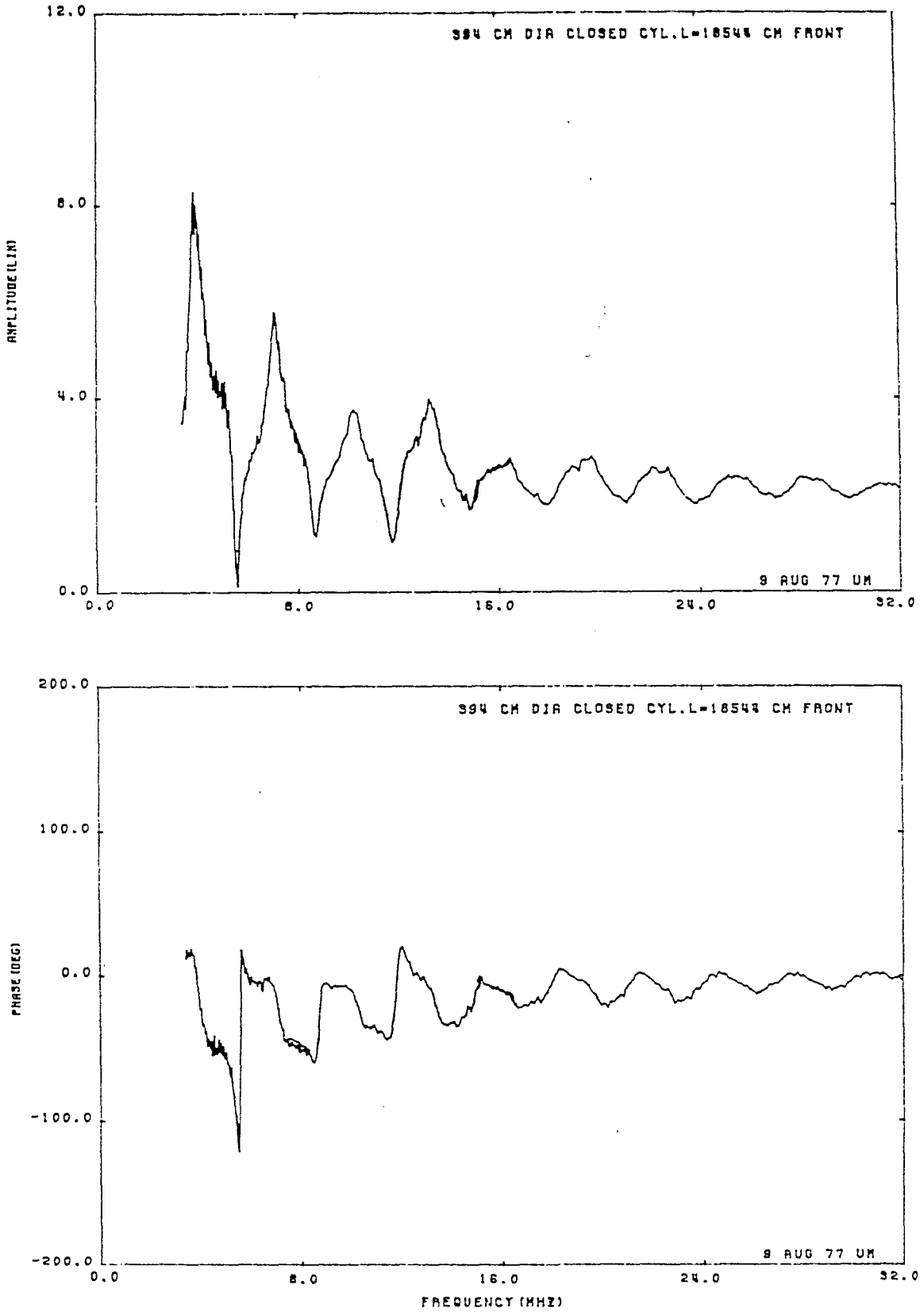

Figure B.13: Current at front center of cylinder No. 3.

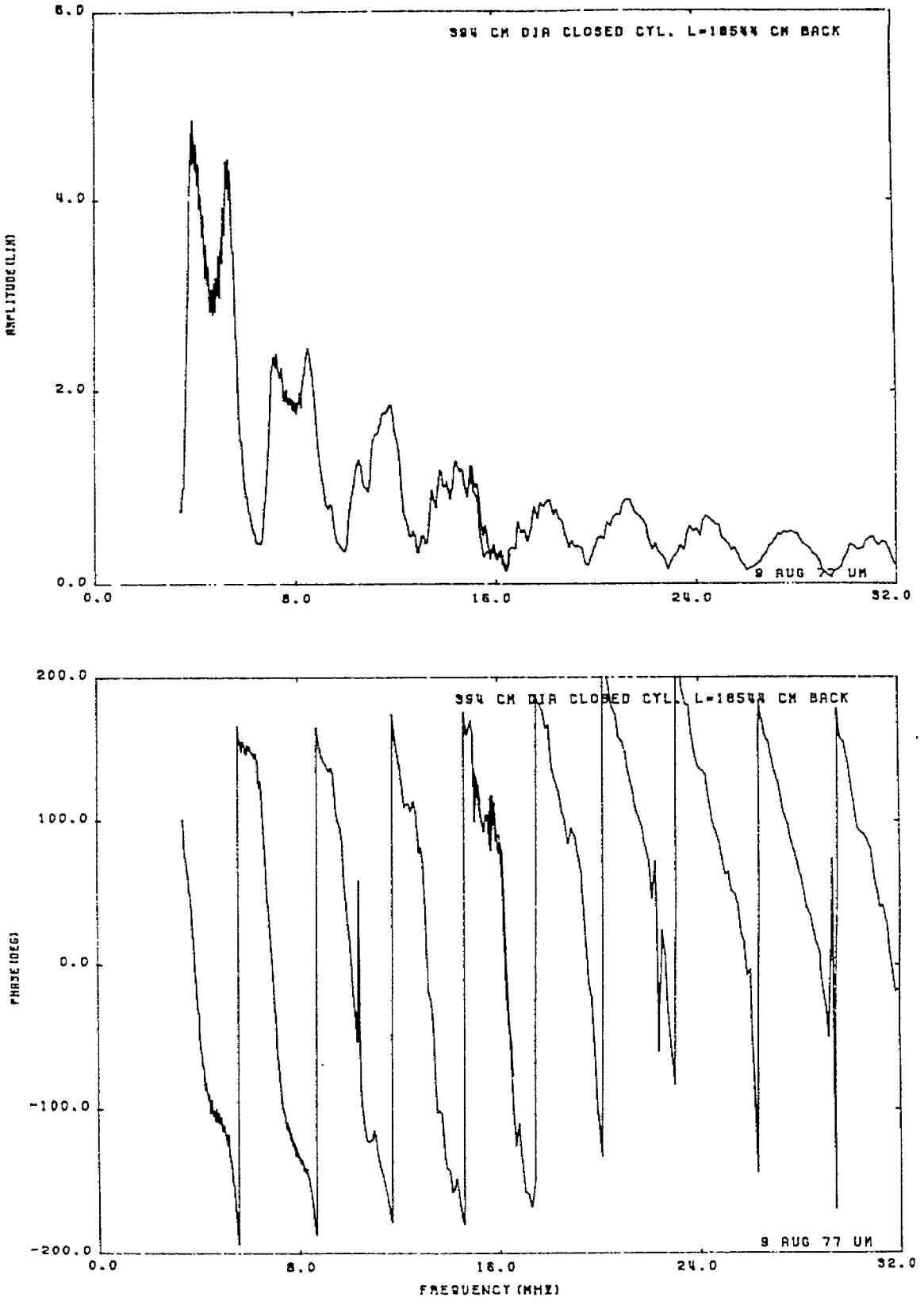

Figure B.14: Current at back center of cylinder No. 3